

**FABRICATION AND PARAMETRIC MEASUREMENTS  
OF N<sub>2</sub> LASER PUMPED DYE LASER AND ITS  
APPLICATION TO ENERGY TRANSFER  
STUDIES IN MIXED DYES**

**P. J. SEBASTIAN**

**THESIS SUBMITTED IN PARTIAL FULFILMENT  
OF THE REQUIREMENTS FOR THE DEGREE  
OF DOCTOR OF PHILOSOPHY**

**UNIVERSITY OF COCHIN  
1981**

CERTIFICATE

Certified that this thesis is the report of the original work carried out by Mr. P.J. Sebastian in the Department of Physics, University of Cochin, under my guidance and supervision and that no part thereof has been included in any other thesis submitted previously for the award of any degree.

Cochin - 22

November 25, 1981.



Professor K. Sathianandan

Supervising Teacher

## ACKNOWLEDGEMENTS

It gives me great pleasure to express my deep sense of gratitude to Dr. K. Mathianandan, Professor and Head of the Department of Physics, University of Cochin, for his able guidance, supervision, encouragement and advice.

I am extremely grateful to all the members of the Faculty, Library, Laboratory and non-teaching staff of the Department of Physics for their co-operation during the course of this work.

I am grateful to Dr. D.D. Bhawalkar and Dr. L.G. Nair, BARC, Bombay, for the discussions with them and for providing some laser dyes.

I owe my sincere thanks to Dr. Girijavallebhan, Dr. V.P.N. Nampoori, Dr. C.P. Menon, Dr. M.G. Krishna Pillai, Subhash, Radhakrishnan, Sudha, Ramachandran, Mohanachandran, Murali, Syam, Vijayakumar, Lizanna, Paul, Reghu and Revishankar for their good wishes and encouragements.

Thanks are also due to the staff members in the C.W.I.S.L., University of Cochin.

My special thanks to Mrs. Suseela, B  
for typing the manuscript.

Finally I take this opportunity to thank  
University of Cochin, U.G.C. and D.C.T. for the timely  
award of fellowships.

Sebastian, P.J.  
Department of Physics  
University of Cochin

## CONTENTS

Page No.

CHAPTER I	ENERGY TRANSFER MECHANISM IN LASER DYES	
1.10	Introduction	1
1.20	Prominent mechanisms of energy transfer	4
1.30	Rate Constants	6
1.40	Effective life time of the acceptor	9
1.50	Kinetic scheme for an ETDL	11
1.60	Organization of the text	13
	References	16
CHAPTER II	FABRICATION OF A DYE LASER PUMPED BY A PULSED $N_2$ LASER	
	Abstract	19
2.10	Pulsed Nitrogen laser as a pump source	20
2.20	General Geometry of dye lasers	22
2.30	Constructional details of a low divergence dye laser	33
2.31	Focussing lens and dye cell	33
2.32	Feedback mirror $M_1$	34
2.33	Grating and tuning mirror $M_2$	35
2.34	Alignment	36
2.35	Performance data	37
2.36	Possible improvements on the design	38
	References	40

CHAPTER III	PARAMETRIC MEASUREMENTS OF THE DYE LASER	
	Abstract	42
3.10	Introduction	43
3.20	Properties of laser dyes	44
3.21	Light absorption	45
3.22	Laser emission and quantum yield of fluorescence	47
3.23	Oscillation condition	50
3.30	Basic parameters of a dye laser	52
3.31	Power output and conversion effi- ciency	57
3.32	Pulse characteristics	57
3.33	Divergence	57
3.34	Bandwidth	63
3.35	Polarization effect due to the $10^\circ$ wedge angle of the dye cell	67
3.36	Tunability	71
	References	76
CHAPTER IV	ENERGY TRANSFER STUDIES IN DYE LASERS	
	Abstract	79
4.10	Introduction	80
4.20	Review of the work on ETDL	80
4.30	Studies on some specific systems and their performance	84

4.31	Rh 6G -- Safranin T	85
4.32	Rh 6G -- Rh B	90
4.33	C 120 -- Rh 6G	102
4.34	Discussion	108
	References	112
CHAPTER V	SUMMARY	116

CHAPTER I

ENERGY TRANSFER MECHANISM IN LASER DYES

## 1.10 Introduction

Many lasers are developed with the faith that yet-to-be discovered applications will justify the expense and the effort of their development. But it is not so with dye lasers; "it was the fulfilment of an experimenter's dream that was as old as the laser itself." The successful demonstration of innumerable applications of dye lasers, soon after the first report on dye lasers by Sorokin and Lankard in 1966, show the importance of dye lasers in almost all the branches of science and technology. Eventhough most of the fixed frequency lasers are much more advanced, the unique features of a dye laser such as wavelength tunability, wide spectral coverage and simplicity, made it more attractive. However, the various applications demand further improvement of the dye lasers in all respects. The developments in the past few years show remarkable progress in improving the tunability, efficiency and power output.

The Ruby laser pumped Chloro-Aluminum-Phthalocyanine dye laser of Sorokin and Lankard<sup>1</sup> demonstrated the feasibility of an organic dye laser. Followed by this sensational discovery many others have experimented with a large number of organic dyes with different pump sources which resulted in a wide spectral coverage of dye lasers ranging from the ultra violet to the near infrared. More precisely

the ultra violet limit of dye laser wavelength obtained so far is 330 n.m. for the dye phenyl-benzoxazole<sup>2</sup> and the infrared limit obtained is 1.24  $\mu$ m. for the dye (4 - [7 - (2 - phenyl - 4H - 1 - benzothiopyran - 4 - Ylidene) - 4 - Chloro - 3, 5 - trimethylene - 1,3,5 - heptatrienyl] - 2 - phenyl - 1 - benzothiopyrylium perchlorate).<sup>3</sup> But many of these dyes are not suitable for CW operation because of the accumulation of dye molecules in the triplet state and thermal and acoustical schlieren effects. The first CW operation of a dye laser was reported by Peterson et al.<sup>4</sup>. They used Rh-6G in water with the addition of some detergent. The detergent acted as a triplet quencher and at the same time prevented dimer formation. During the pumping process a thermally induced refractive index gradient is set up in the dye solution. Since water is much less sensitive to this effect compared to organic solvents it acts as a good solvent for CW dye lasers. But unfortunately many dyes are insoluble in water. The attempts made to synthesize new water soluble dyes for CW operation are encouraging.<sup>5,6</sup>

Many of the potential advantages of dye lasers are defeated by the lack of an efficient, reliable and inexpensive pump source. Most of the pump laser sources used for CW and pulsed operation of dye lasers are very expensive. The relatively inexpensive pulsed N<sub>2</sub> lasers can be reliable but are rather inefficient. However, since the first report

of  $N_2$  laser pumped dye laser by Hayer et al.<sup>7</sup> the potential use of  $N_2$  laser as a pump source was demonstrated by many others. Sorokin and Lankard<sup>8</sup> demonstrated the use of flash lamps, comparable in rise time and intensity to giant pulse ruby lasers, as pump sources for dye lasers. Eventhough flash lamps allow simple design of dye lasers their short life time for operation at high repetition rates make it uneconomical.

Under these circumstances it was quite natural to put efforts to enhance the conversion efficiency of  $N_2$  laser pumped dye lasers. The  $N_2$  laser pumped gaseous phase dye laser operation reported shows better efficiency.<sup>9,10</sup> Recently Marowsky et al.<sup>11</sup> successfully tried electron beam pumped vapour phase dye lasers. Although these methods can give more efficient dye lasers, they are more expensive. A similar expensive but efficient method is to use an oscillator - amplifier system as described by Itzkan and Cunningham.<sup>12</sup> They obtained a conversion efficiency of 25%. A large number of dye laser geometry have been tried with the intention of getting enhanced efficiency.<sup>13-15</sup> Eventhough some of them<sup>15</sup> make the system more simple the efficiency enhancement is not appreciable.

A widely accepted inexpensive method for increasing the efficiency of dye laser is the energy transfer

mechanism. Since the first report of Keller et al.<sup>15</sup> on enhancement of pumping efficiency in  $N_2$  laser pumped dye laser by energy transfer mechanism the technique has been a subject of intense study. The studies on energy transfer dye laser (ETDL) systems help not only to optimize the system but also to get an understanding of the photo-reactions of the dye molecules. Energy transfer mechanism enables laser action from dyes which are difficult or even impossible to pump above threshold with the  $N_2$  laser. Thus the spectral coverage of  $N_2$  laser pumped dye lasers can be extended by energy transfer mechanism. The present investigations mainly pin points various performance characteristics of ETDL systems. The theoretical aspects of energy transfer mechanism in relation to the present investigations are discussed briefly in the following sections of this chapter.

### 1.20 Prominent Mechanisms of Energy Transfer

The main mechanisms for the intermolecular singlet - singlet electronic energy transfer in dye mixtures are (1) radiative transfer - emission of donors absorbed by acceptors (2) diffusion controlled collisional transfer and (3) resonance transfer. Mechanisms 2 and 3 are also called non radiative transfer. Mechanism 3 occurs with the donor-acceptor separation much greater than the collisional diameters. The origin of resonance transfer is the long-range

dipole - dipole coulomb interaction. The probability of energy transfer due to such interaction is large if the emission spectrum of the donor strongly overlaps the absorption spectrum of the acceptor, a condition necessary for radiative transfer also. Collisional transfer is an excitation transfer process which requires close approach of donor and acceptor in order to obtain efficient transfer. If every collision between excited donor and acceptor molecules leads to transfer, the transfer rate will be the diffusion controlled rate. The radiative transfer involves the possibility of reabsorption of donor emission. The process requires two steps with the intermediacy of a photon. No direct interaction is involved. Obviously only energies corresponding to that part of the emission spectrum of the donor that overlaps the absorption of the acceptor can be transferred. The transfer efficiency is governed by quantum yield of fluorescence of donor and by Beer-Lambert law. The probability that an acceptor reabsorbs the light emitted by a donor at a distance  $R$  varies as  $R^{-2}$ .

Although all these mechanisms contribute to the donor fluorescence quenching and enhance the acceptor fluorescence yield, they can be distinguished experimentally. The radiative transfer does not affect the donor fluorescence life time where as the other two processes affect the life time. The diffusion controlled collisional transfer rate

is inversely proportional to the solvent viscosity while radiative and resonance transfer rates are independent of solvent viscosity. Also, theory and experiments suggest that resonance transfer rate is atleast ten times faster than collisional transfer rate. Thus the study of donor fluorescence life time as a function of acceptor concentration and solvent viscosity can distinguish the various mechanisms.

### 1.30 Rate Constants

The bimolecular process of energy transfer between donor and acceptor can be represented by



The rate constant  $K_{et}$  may be associated with the diffusion controlled kinetic processes which in turn is associated with the short range exchange interaction of the Dexter type. In such a case<sup>17</sup>

$$K_{et} = \frac{8 RT}{3000 \eta} \dots (1.1)$$

where  $\eta$  is the viscosity of the medium. But this is a relatively slow process to effectively compete with the fluorescence decay of  $D^*$  molecules in ETDL systems.

A faster transfer process is that due to long range dipole - dipole interaction of Forster type. The

rate constant for the process is given by<sup>13</sup>

$$K_{et} = \frac{3.8 \times 10^{-25} K^2 \phi_D}{n^4 \tau_D R^6} \int_0^{\infty} F_D(\nu) \epsilon_A(\nu) \frac{d\nu}{\nu^4} \quad \dots (1.2)$$

where  $\nu$  is the wave number,  $F_D(\nu)$  is the spectral distribution of the donor emission in quanta normalized to unity,  $\epsilon_A(\nu)$  is the molar extinction coefficient for the acceptor absorption,  $n$  is the refractive index of the solvent,  $K$  is an orientation factor equal to  $(2/3)^{1/2}$  for a random distribution of donor and acceptor molecules,  $\phi_D$  is the quantum yield of donor emission,  $\tau_D$  is the observed donor emission life time in the presence of acceptor and  $R$  is the distance between donor and acceptor molecules.

The efficiency of Forster type energy transfer is usually expressed in terms of a critical distance  $R_0$ , the separation of donor and acceptor at which the rate of energy transfer is equal to the sum of the rates of all other donor deexcitation processes. In other words

$$K_{et}(\text{at } R_0) = \frac{1}{\tau_D} \quad \dots (1.3)$$

$$\text{and } R_0^6 = \frac{3.8 \times 10^{-25} K^2 \phi_D}{n^4} \int_0^{\infty} F_D(\nu) \epsilon_A(\nu) \frac{d\nu}{\nu^4} \quad \dots (1.4)$$

The critical concentration of acceptor  $C_A^o$  at which the transfer is 50% efficient (the donor fluorescence is half quenched) is given by

$$C_A^o \text{ (moles/liter)} = \frac{4.8 \times 10^{-10} n^2}{K} \left[ \Phi_D \int_0^\infty F_D(\nu) \epsilon_A(\nu) \frac{d\nu}{\nu^4} \right]^{-1/2} \dots (1.5)$$

$$\text{and } R_o(A^o) = \frac{7.35}{(C_A^o)^{1/3}} \dots (1.6)$$

The rate constant  $K_{et}$  can be experimentally determined from Stern-Volmer relation also which states

$$\frac{\tau_{fo}}{\tau_f} = 1 + K_{et} A \tau_{fo} \dots (1.7)$$

Where  $\tau_{fo}$  is the measured life time of the donor in the absence of acceptor molecules and  $\tau_f$  that in the presence of acceptor.  $A$  is the acceptor concentration. From a plot of  $1/\tau_f$  Vs.  $A$  we can obtain  $A_{1/2}$  the acceptor concentration at which  $\tau_f = 1/2 \tau_{fo}$ .  $K_{et}$  is then calculated from

$$K_{et} A_{1/2} = (\tau_{fo})^{-1} \dots (1.8)$$

By knowing  $A_{1/2}$  we can calculate  $R_o$  from

$$R_o = 7.35 (A_{1/2})^{-1/3} \dots (1.9)$$

#### 1.40 Effective Life Time of the Acceptor

The effective fluorescence life time of the acceptor in a dye mixture changes due to energy transfer reaction which causes a change in the gain spectrum.<sup>21</sup> A rate equation analysis of the donor acceptor laser dye mixture gives the extend of this change in the life time. The rate equations are given by

$$\frac{dN_{1d}}{dt} = c\bar{q} N_{0d} \sigma_d(\lambda_0) - \frac{N_{1d}}{\tau_d} - K_{da} N_{1d} N_{0a} \quad \dots (1.10)$$

$$\text{and } \frac{dN_{1a}}{dt} = c\bar{q} N_{0a} \sigma_a(\lambda_0) - \frac{N_{1a}}{\tau_a} + K_{da} N_{1d} N_{0a} + K'_{da} N_{1d} N_{0a} - K_{nr} N_{1a} N_{0d} \quad \dots (1.11)$$

in which the induced emission and triplet state contributions are neglected. Suffixes a and d represent acceptor and donor.  $N_1$  and  $N_0$  are the concentration of first excited singlet state and ground state molecules  $\bar{q}$  is the average photon density of the pump laser in the active region,  $\sigma(\lambda_0)$  absorption cross section at pump wavelength and  $\tau$  is the life time of pure solutions of donor or acceptor. Rate constant  $K'_{da}$  is for radiative transfer  $K_{da}$  for resonance

transfer and  $K_{nr}$  for quenching process of the excited acceptor due to collisions with the ground state donor molecules.

The average photon density  $\bar{q}$  is given by

$$c\bar{q} = (P_0/\delta L) [1 - \exp(-1)] \quad \dots (1.12)$$

where  $P_0$  is the input pumping power,  $\delta$  is the width of the focussed pumping beam and  $L$  is the length of the active region.

From stationary state approximation

$$\frac{dN_{1d}}{dt} = 0 \text{ and } \frac{dN_{1a}}{dt} = 0 \quad \dots (1.13)$$

Then from eq. (1.12) and (1.13) we get

$$N_{1a} = \frac{W\tau_a}{1 + K_{nr}\tau_a N_{od}} \left( 1 + \frac{\beta(K_{da} + K'_{da})N_{od}}{1/\tau_d + K_{da}N_{oa}} \right) N_{oa} \quad \dots (1.14)$$

where  $\beta = \frac{\sigma_d(\lambda_0)}{\sigma_a(\lambda_0)}$  and  $W = \frac{P_0 [1 - \exp(-1)] \sigma_a(\lambda_0)}{L}$

The intensity of the gain coefficient.

$$g(\lambda) = -N_{oa}\sigma_{abs}(\lambda) + N_{1a}\sigma_{em}(\lambda) \quad \dots (1.15)$$

from (1.14) and (1.15) we get

$$g(\lambda) = \nu(\lambda) N_{oa}$$

$$\text{Where the gain coefficient } \nu(\lambda) = -\sigma_{ab}(\lambda) + W\tau_{ef}\sigma_{em}(\lambda) \quad \dots (1.16)$$

$$\text{and } \tau_{ef} = \frac{\tau_a}{1+K_{nr}\tau_a N_{od}} \left( 1 + \frac{\beta(K_{da} + K'_{da})N_{od}}{1/\tau_d + K_{da} N_{oa}} \right) \quad \dots (1.17)$$

is the effective life time of the acceptor.

#### 1.50 Kinetic Scheme for an ETDL

The Kinetic scheme corresponding to the singlet manifolds of donor and acceptor coupled by dipole - dipole interaction is shown in Fig. 1.1<sup>22</sup>. This scheme can be utilized to analyse the dynamic characteristics of an ETDL.  $K_{DA}^1(10) [A_o]$  and  $K_{DA}^1(20) [A_o]$  are the rates of energy transfer from  $S_1$  and  $S_2$  states of donor. Each manifold is pumped with a source of intensity  $I_p$  at a rate  $\sigma_{01}(P) I_p$ . Photoquenching processes (20) in donor and acceptor manifolds are represented by the rates  $\sigma_{12}(P) I_p$ . Lasing occurs in the acceptor at the rate of  $\sigma_e I_L$ . Where  $I_L$  is the dye laser intensity generated and  $\sigma_e$  is the cross section for stimulated emission. Absorption losses at the dye laser



frequency are represented by the rate constants  $\sigma_{01}^A(L) I_L$  and  $\sigma_{12}^A(L) I_L$ . Radiationless decay rate processes are given by  $K_{ij}$ .

For an ETDL where photoquenching effects are negligible, the low signal gain for an ETDL operating near threshold is given by<sup>23</sup>

$$G = \left[ \sigma_e - \sigma_{12}^A(L) \right] \sigma_{01}^A(P) \tau_a \left( \frac{R_0}{R} \right)^6 I_p [A] [D] \\ \times \left\{ 1 + \left( \frac{R_0}{R} \right)^6 + \tau_D \sigma_{01}^D(P) I_p [A] \right. \\ \left. + \tau_a \sigma_{01}^D(P) I_p \left( \frac{R_0}{R} \right)^6 [D] \right\}^{-1/2} - \sigma_{01}^A(L) [A] \quad \dots (1.18)$$

The above gain expression shows that ETDL performance can be manipulated by varying the donor or acceptor concentrations.

## 1.60 Organization of the Text

Chapter I of this text is introductory. While Chapter II deals with a comparative study of the various commonly accepted designs of  $N_2$  laser pumped dye lasers followed by a discussion on the importance of  $N_2$  laser as a

pump source. The constructional details of the  $N_2$  laser pumped dye laser fabricated for the present investigations are also discussed.

Chapter III deals with the measurements on the various beam qualities of the output beam and their dependence on various system parameters. The following aspects are covered in this section.

1. Output power variation with input power as well as bandwidth.
2. Pulse shape and duration.
3. Divergence of the beam as a function of distance between dye cell and feedback mirror.
4. Bandwidth as a function of angle of incidence of grating as well as divergence.
5. Tunability.
6. Polarization effects in the output beam as a result of the  $10^\circ$  wedge angle given to the dye cell.

Chapter IV gives a general picture of the ETDL systems. The chapter begins with brief review on ETDL systems. The results of the investigations on the performance

characteristics of three specific EFDL systems, Rh-6G - Safranin T, Rh-6G - Rh-B and C 120 - Rh-6G, are discussed in detail. The discussions are mainly centered on the spectral shifts and efficiency of EFDL systems. However, a partial coverage of the aspects such as tunability, Polarization and excited state reactions have also been made. Chapter V is the summary.

References

1. P.P. Sorokin and J.R. Lankard, IBM J. Res. Dev. 10, 162 (1966).
2. C. Rulliere and J.J. Dubien, Opt. Commun, 24, 38 (1978).
3. W. Kranitzky, B. Kopainsky, W. Kaiser, K.H. Drexhage and G.A. Reynolds, Opt. Commun. 36, 149 (1981).
4. O.G. Peterson, S.A. Tuccio and B.E. Snavely, Appl. Phys. Letters. 17, 245 (1970).
5. S.A. Tuccio, K.H. Drexhage and G.A. Reynolds, Opt. Commun. 7, 248 (1973).
6. K.H. Drexhage, G.R. Erikson, G.H. Hawks and G.A. Reynolds, Opt. Commun. 15, 399 (1975).
7. J.A. Meyer, C.L. Johnson, E. Klerstead, H.D. Sharma and I. Itzkan, Appl. Phys. Letters, 16, 3 (1970).
8. P.P. Sorokin and J.R. Lankard, IBM J. Res. Dev. 11, 148 (1967).
9. B. Steyer and F.P. Schafer, Opt. Commun. 10, 219 (1974).
10. P.W. Smith, P.F. Liao, C.V. Shank, C. Lin and P.J. Maloney, Appl. Phys. Letters. 25, 144 (1974).

11. F.P. Schafer, High power lasers and applications, eds. K.L. Kompa and H. Walther. (Springer-Verlag 1978), p. 114.
12. I. Itzkan and F.W. Cunningham, IEEE J QE - 8, 101 (1972).
13. T.W. Hansch, Appl. Opt. 11, 895 (1972).
14. D.C. Hanna, P.A. Karkkainen and R. Wyatt, Opt. Quant. Electr. 7, 115 (1975).
15. M.G. Littman and H.J. Metcalf, Appl. Opt. 17, 2224 (1978).
16. C.E. Holler, C.W. Verber and A.M. Adelman, Appl. Phys. Letters. 13, 278 (1971).
17. A.L. Lamola and N.J. Turro, Energy Transfer and Organic Photochemistry (Interscience - New York - 1969) p. 34.
18. A.L. Lamola and N.J. Turro, Energy Transfer and Organic Photochemistry (Interscience - New York - 1969) p. 37.
19. A.L. Lamola and N.J. Turro, Energy Transfer and Organic Photochemistry (Interscience - New York - 1969) p. 82.

20. A.J. Pesece, C.G. Rosen and L. Pasby, Fluorescence Spectroscopy (Marcel Dekker Inc. New York - 1971) p. 92.
21. T. Urisu and K. Kajiyama, J. Appl. Phys. 47, 3563 (1976).
22. S. Speiser and R. Katrarro, Opt. Commun. 27, 287 (1978).
23. E. Weiss and S. Speiser, Chem. Phys. Letters, 42, 220 (1976).

CHAPTER II

FABRICATION OF A DYE LASER PUMPED BY  
A PULSED N<sub>2</sub> LASER

ABSTRACT

The relative merits and demerits of different dye laser schemes are discussed. The constructional details of a narrow band and low divergence dye laser pumped by a  $N_2$  laser is presented. The beam divergence is reduced by adjusting the distance between the feedback mirror and the dye cell. The system gives an output peak power of 15 kW at a bandwidth of  $0.9 \text{ \AA}^{\circ}$ . The divergence of the output beam is 2 mrad.

## 2.10 Pulsed Nitrogen Laser as a Pump Source

The output of the Nitrogen laser has been shown to be a convenient pump source for a wide variety of dye lasers.<sup>1</sup> The fluorescence band of a dye solution as a result of the transition from the lowest vibronic level of the first excited singlet state to some higher vibronic levels of the ground state is utilized in a dye laser. . But the existence of the lower lying triplet states deteriorate the system performance. The intersystem crossing rate to the lowest triplet state is high enough in most molecules to reduce the quantum yield of fluorescence to values appreciably below unity. This reduces the population of the excited singlet state and hence the amplification factor and also it enhances triplet-triplet absorption losses of both the pump light and the laser emission. A simple calculation can demonstrate the importance of triplet states in dye lasers.<sup>2</sup> At steady state the rate of triplet formation becomes equal to the rate of deactivation and is represented by

$$P\sigma n_0\phi_T = \frac{n_T}{\tau_T} \quad \dots (2.1)$$

where  $P$  is the pump flux density,  $\sigma$  total molecular absorbing cross-section,  $\phi_T$  quantum yield of triplet formation,  $n_0$  and  $n_T$  the populations of the ground and triplet states

respectively and  $\tau_T$  the triplet life time. Thus the fraction of the molecules in the triplet state is

$$\frac{n_T}{n} = \frac{P_0 \sigma_T \tau_T}{(1 + P_0 \sigma_T \tau_T)} \quad \dots (2.2)$$

Assuming typical values for a dye,  $\sigma = 10^{-16} \text{ cm}^2$ ,  $\phi_T = 0.1$ ,  $\tau_T = 10^4 \text{ Sec.}$ , it can be seen that to maintain half of the molecules in the triplet state the power required is  $P_{1/2} = 1/2 \text{ kW cm}^{-2}$ ; a much smaller quantity than the threshold pump power required. Hence a slowly rising pump light flux density transfers most of the molecules to the triplet state. But if the pump light pulse rises fast such that it reaches threshold in a time  $t \ll \frac{1}{K_{ST}}$  (reciprocal of the intersystem crossing rate) the population of the triplet level can be held arbitrarily small. A typical value of  $K_{ST}$  for a dye is  $10^7 \text{ Sec.}^{-1}$ . Thus if  $t \ll 100 \text{ nsec}$  the triplet effects can be neglected. The 10 nsec  $\text{N}_2$  laser pulse can thus avoid the triplet influences in a dye laser.

The absorption coefficient of most organic dyes at 337.1 nm is sufficient to pump above threshold to get laser action. The wavelength region of laser action that can be obtained from  $\text{N}_2$  laser pumping covers the range 355 to 940 nm.<sup>1</sup> For example, the dye PBD gives 355 nm and Dibenzocyanin 45 gives 940 nm laser radiation by  $\text{N}_2$  laser pumping. Thus a

short duration  $N_2$  laser is a very attractive source for the pumping of dye lasers with a wide range of frequencies.

## 2.20 General Geometry of Dye Lasers

A large number of arrangements have been developed for narrow band, low divergence, high conversion efficiency and tunable  $N_2$  laser pumped dye lasers.<sup>3-23</sup> The key element determining the quality of the dye laser is the beam expander. The commonly used beam expanding devices are telescopes,<sup>3,4</sup> single and multiple prisms<sup>5-10</sup> and grating at grazing incidence<sup>11-15</sup>. A critical evaluation of the performance data of these different designs and their relative merits and demerits is helpful in designing a dye laser system for a particular application. An attempt in this direction is recently reported<sup>24</sup> but the comparative study is limited to prism and grazing incidence grating beam expanders.

Essentially the dye laser cavity consists of the active medium (the dye solution in a cell), the feedback element, mechanism for beam expansion and the tuning element. Hansch<sup>3</sup> has described a dye laser system which incorporates a diffraction grating as the tuning element, a high power beam expanding telescope to expand the laser beam and fill the grating with a collimated beam and a partially reflecting

feedback mirror. The schematic of the system is shown in Fig. 2.1. The 4% reflecting plane glass plate is used as the feedback and outcoupling element. A 20 X beam expanding telescope in autocollimation and a diffraction grating at an angle of incidence  $60^\circ$  in Littrow mount is used for spectral narrowing. Lawler et al.<sup>4</sup> have estimated the single pass bandwidth  $\Delta\lambda_{1/2}$  (FWHM) of the system by modeling the laser as a slit spectrometer. The transverse dimensions of the tiny cylindrical region of the excited dye in the direction perpendicular to the rulings of the grating is the limiting aperture of the spectrometer. The entrance and exit apertures are considered to be located at the centre of the dye cell since the telescope is used in autocollimation. The dispersion of the grating in Littrow mount is

$$\frac{d\theta}{d\lambda} = \frac{2 \tan \theta}{\lambda} \quad \dots (2.3)$$

Then the linear dispersion in the plane of the exit slit is

$$F \frac{d\theta}{d\lambda} = 2 F \frac{\tan \theta}{\lambda} \quad \dots (2.4)$$

Where F is the thick lens focal length of the telescope given by

$$F = \left( \frac{1}{f_1} + \frac{1}{f_2} - \frac{s}{f_1 f_2} \right)^{-1} = - (d - f_1) (f_2 / f_1) \quad \dots (2.5)$$

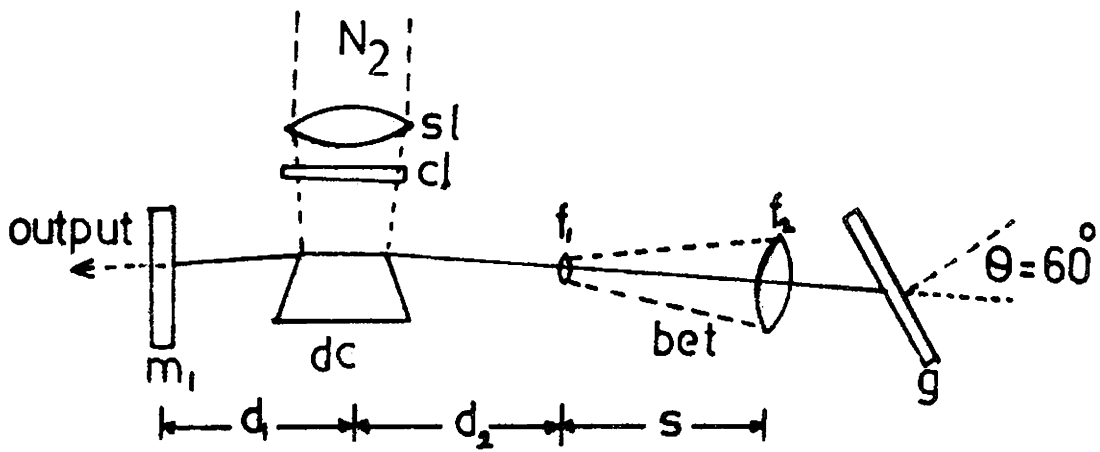


Fig.2.1. Configuration of dye laser as suggested by Hansch.

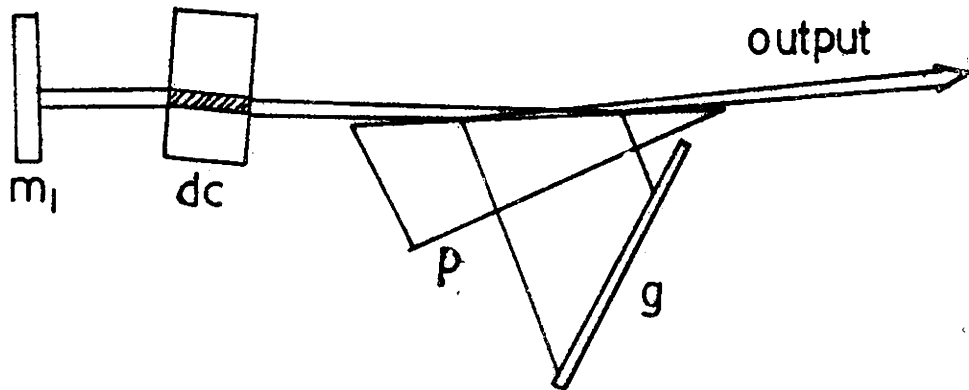


Fig.2.2. Configuration of dye laser with prism beam expander.

Where  $d_2$  is the air equivalent path length between the centre of the dye cell and the eye piece of the telescope,  $f_1$  and  $f_2$  are the focal lengths of the eye piece and the objective respectively. The limit of resolution of the slit spectrometer is given by

$$\Delta\lambda_{1/2} = \Delta_{1/2} \left[ 2 (d_2 - f_1) (f_2/f_1) \frac{\tan \theta}{\lambda} \right] \dots (2.6)$$

Where  $\Delta_{1/2}$  is the FWHM of the instrument profile function which is the convolution of the exit aperture with the image of the entrance aperture as it is focussed at the exit slit.

In a real spectrometer, when the grating is not overfilled, the instrument profile is the convolution of the exit and entrance slits. If the grating is overfilled, the image of the entrance aperture can be broadened by diffraction. For the dye lasers the excited region is not sharp edge slits but are characterised by grey edges. Hence to obtain the profile function, we have to determine the transmittance function of the equivalent slits. The convolution of the transmittance function with itself gives the profile function. The feedback laser beam can be approximated by a Gaussian profile and hence a similar shape for the transmittance function. The convolution of the Gaussian transmittance function with itself (the half width of the instrument profile) is given by

$$\Delta_{1/2} = \frac{0.627\lambda}{\Delta\theta_{1/2}} \quad \dots (2.7)$$

Where  $\Delta\theta_{1/2}$  is the measured angular width of the Fraunhofer diffraction pattern (FWHM) of the feedback laser beam. Lawler et al.<sup>4</sup> found from the measured pattern that the function  $\exp[-1 \times 4\pi\Delta\theta_{1/2}/1.28\lambda]$  is a better fit for the transmittance function. In this case

$$\Delta_{1/2} = \frac{0.25\lambda}{\Delta\theta_{1/2}} \quad \dots (2.8)$$

The nature of the excited region of the dye and hence the transmittance function depends on the  $N_2$  laser power, the details of the focussed  $N_2$  beam and the dye concentration. Lawler et al.<sup>4</sup> have obtained the above experimental fit for  $\Delta_{1/2}$  with  $5 \times 10^{-3}$  M solution of 7D4 MC in ethyl alcohol and the  $N_2$  beam being focussed by a single 12 cm focal length lens. They observed a reduction in the angular divergence of the feedback laser beam when N power was decreased from 0.5 MW to 0.1 MW and an improvement in the bandwidth by a factor of two.

A close examination of the operation of the dye laser reveals some of the drawbacks of the design of Hansch,<sup>3</sup> introduced due to its relatively large cavity length ( $\sim 60$  cm). During the beginning of the  $N_2$  pulse, some light emitted by the

excited dye is directed to the feedback mirror. A fraction of this light is reflected back to the excited dye where it is amplified and emerges in the direction of the telescope. This feedback beam is expanded and collimated by the telescope. The grating disperses this light and a narrow band is reflected back to the active medium for amplification for the second time. This narrow band amplified beam comes out as the laser radiation. It is clear that there is a time delay of at least  $\frac{2L}{c}$  between the beginning of  $N_2$  pulse and the dye laser pulse. This time delay can be greater than  $\frac{2L}{c}$  if  $N_2$  laser power is either low or turns on slowly. Hence for efficient pumping  $\frac{2L}{c}$  should be much less than  $N_2$  pulse duration. Further more if  $N_2$  pulse power is very high and if the narrow band radiation is not quickly returned to the dye cell for final amplification, there will be troublesome loss mechanisms like superradiance and photo-excitation from the excited states to higher levels. From the above discussions it is clear that for efficient operation of a dye laser a short cavity is needed.

A short cavity can be obtained by decreasing the distance between dye cell and feedback mirror ( $d_1$ ), the distance between dye cell and eye piece of the telescope ( $d_2$ ) and power of the telescope. But all these steps increase the bandwidth. If the feedback mirror is too close to the dye cell the divergence of the feedback beam will be greater than the diffraction limit which results in an increase in bandwidth.

A reduction in  $d_2$  or magnification of telescope ( $M = f_2/f_1$ ) increases  $\Delta\lambda/2$  as can be seen from equation 2.6. The power of the telescope can be kept low by selecting a small focal length negative lens for the eyepiece thereby reducing the length of the telescope. But negative lenses of focal length less than a few mm are not available.

But as suggested by Lawler et al.,<sup>4</sup> if a low power telescope is used with the grating at larger angle of incidence the bandwidth can be kept small and at the same time reduce the cavity length. A bandwidth of 0.01 nm and conversion efficiency (the ratio of dye laser power to  $N_2$  laser power) of 10% can be obtained by this method. But for a low bandwidth of 0.001 nm the insertion of an intracavity etalon between the telescope and the grating is necessary. But it results in lowering the efficiency to  $\sim 1\%$ . The efficiency can be improved to  $\sim 3\%$  by reshaping the  $N_2$  laser pump pulse, that is by allowing a small fraction of  $N_2$  power to fall on the dye cell first and after a time delay of  $\frac{2L}{c}$  the rest of the  $N_2$  power; thereby the system acts first as an oscillator and then as an amplifier.<sup>4</sup>

The use of a telescope as a beam expander in a dye laser system is not attractive owing to its high cost and difficulty in alignment. Moreover, the high cavity length of the dye laser with telescope beam expander does not permit pumping with very short duration pulses. Hanna et al.<sup>5</sup> used

a prism as the beam expander as shown in Fig. 2.2 and obtained linewidth and efficiency comparable with telescope beam expander and a shorter cavity.

But a more attractive cavity design for  $N_2$  laser pumped dye laser is given by Shoshan et al.<sup>11</sup> The narrow band operation of the dye laser is achieved by using a grating near grazing incidence as the beam expanding device. The schematic of the design is shown in Fig. 2.3. The angular dispersion obtained with the grating mirror combination is given by

$$\frac{d\theta}{d\lambda} = \frac{2m}{a \cos\theta} \quad \dots (2.9)$$

Where  $m$  is the diffraction order,  $a$  is the groove spacing of the grating and  $\theta$  is the angle of the diffracted beam. This angular dispersion is twice as large as that obtained in the usual Littrow arrangement because the beam is diffracted twice before returning to the dye cell. The illumination of the grating near grazing incidence allows the whole width of the grating being illuminated and thus satisfies the condition for highest resolution obtainable with a grating. The single pass bandwidth is given by

$$= 2 \frac{\Delta\omega}{(d\theta/d\lambda)} = \frac{a \cos\theta \Delta\omega}{m} \quad \dots (2.10)$$

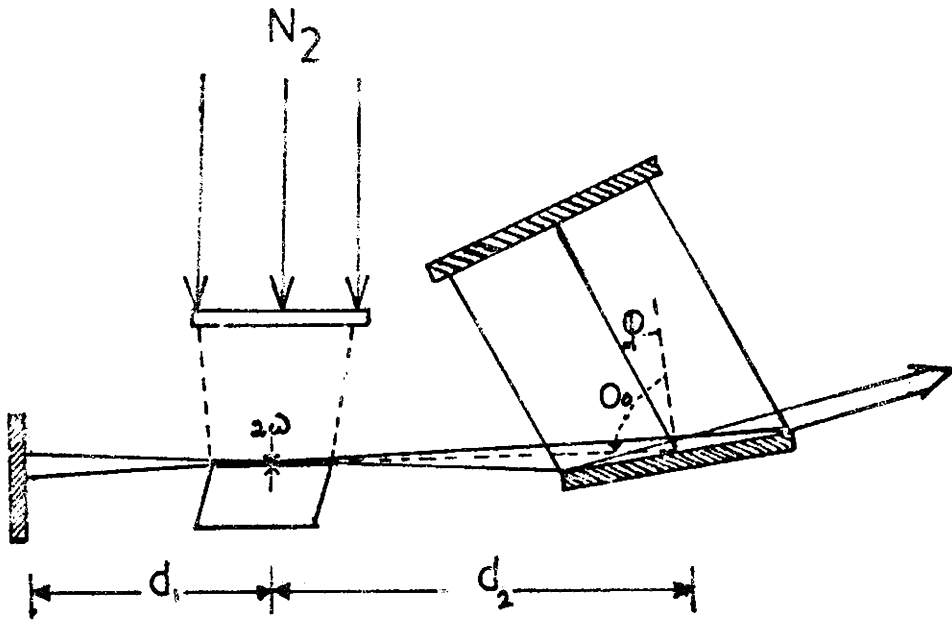


Fig.2.3. Schematic of dye laser with grazing incidence grating beam expander.

Where  $\delta\omega$  is the half angle divergence of the super fluorescent beam incident on the grating. Instead of reducing  $\delta\omega$  by beam expansion, Shoshan proposed the method of increasing  $\frac{d\theta}{d\lambda}$  by increasing angle to obtain a smaller bandwidth. But the diffraction efficiency of grating at very high angle of incidence is very low. However, efficient lasing is possible even with such low feedback from the grating since the cavity length is small and a 100% reflecting mirror is used in the place of the 4% window used by Hansch et al.<sup>3</sup> The small cavity length permits more number of light passes and the 100% mirror provides a more intense feedback to the grating. The grazing incidence grating dye laser design of Littman et al.<sup>12</sup> using a 4% reflecting feedback mirror is not attractive. The 4% mirror does not give sufficient feedback to the grating and hence the feedback from the grating to the dye cell for final amplification of the narrow band is not sufficient if the grating is not of high efficiency. But the 100% mirror provides an intense feedback to the grating and as a result the grating feedback will also be intense. This enables the use of an even low efficiency grating and gives a wider tuning range from a given dye solution.

A grating with many diffraction orders may cause undesirable direct feedback from it to the dye cell when the equation for the Littrow arrangement ( $2a \sin \theta = m\lambda$ ) is satisfied for an order higher than the one used. If a grating

with a groove spacing satisfying  $1/2\lambda < a < \lambda$  is used in first order, only a single diffraction order exists and the undesired feedback to the dye cell can be avoided. The multiple reflections between grating and Mirror  $M_2$  can be eliminated by mounting the grating so that the grooves are not exactly perpendicular to the optical axis of the laser. The tuning element and the Mirror  $M_2$  must be positioned accurately. The zeroth order reflected component from the grating is taken as the output.

The dye laser design without a beam expander has many advantages. The absence of telescope or prism expander makes the alignment more simple and cavity length can be kept small so that short duration pump pulses can be used more effectively. The number of reflecting and transmitting surfaces in the cavity is minimized resulting in less losses. At the same time the performance of the design is comparable or even better than with other designs employing beam expanding devices in the cavity. Table I shows the relative performance data of different dye laser designs.

Table I

Design	Efficiency	Bandwidth	Divergence	Cavity length
Hansch <sup>3</sup>	3%	.03 A <sup>0</sup>	2.5 mrad	40 cm
Lawler <sup>4</sup>	10%	.15 "	1.2 "	15 "
Hanna <sup>5</sup>	7.5%	.1 "	1 "	10 "
Shoshan <sup>11</sup>	8%	.03 "	1 "	15

### 2.30 Constructional Details of a low Divergence Dye Laser

Considering the various advantages of the dye laser design of Shoshan et al.,<sup>11</sup> a similar dye laser system was fabricated for the present investigation. The 337.1 nm radiation from an N<sub>2</sub> laser (CEL Model 101, 200 kW peak power, 30 pps) was used as the pumping source.

### 2.31 Focussing Lens and Dye Cell

A 10 cm focal length cylindrical quartz lens focusses the N<sub>2</sub> laser beam at 11.5 cm away from the lens into a line image of 2.2 cm length. Because of the divergence of the N<sub>2</sub> laser beam the focal point was shifted by 1.5 cm. The lens

was mounted on a precision lens mount with arrangements to adjust the vertical and horizontal tilt angles. A UV spectrometer quartz cell (10 X 10 X 40 mm) with all the sides polished to a high accuracy and with a tight fit cap was mounted on a translation stage. This stage can provide two dimensional positioning and an angular tilt to the dye cell. The dye cell was so positioned that the focussed  $N_2$  laser beam falls just on the inner side of the cell wall and that the parallel end windows of the dye cell make an angle  $10^\circ$  with respect to the dye laser axis to prevent etalon effects at the cell walls.

### 2.32 Feedback Mirror $M_1$

The feedback mirror  $M_1$  shown in Fig. 2.3 was a back surface aluminium coated mirror (Reflectivity  $\sim 90\%$ ) on a highly polished (surface accuracy  $\lambda/10$ ) glass substrate. Eventhough the alignment of the laser is unusually simple and relatively insensitive to pump laser focus and grating position it is quite sensitive to the path through the dye cell as determined by this feedback mirror. Hence this mirror had to be mounted on a quality mirror mount. The resolution of the mirror mount used was 5 sec of arc. Moreover the distance of this mirror from the centre of the dye cell can control the beam divergence of the dye laser. In order to get a

diffraction limited beam divergence this mirror had to be positioned at a distance of 8 cm from the centre of the dye cell. But this increases the cavity length and thereby decreases the efficiency of the laser. Hence as a compromise the mirror  $M_1$  was positioned at 5 cm from the cell and then the divergence of the dye laser beam was  $\sim 2$  mrad.

### 2.33 Grating and Tuning Mirror $M_2$

A 30 mm wide, 1800 l/mm Bausch and Lomb grating was used at grazing incidence. (angle of incidence  $88^\circ$ ). The blaze wavelength of the grating was  $5000 \text{ \AA}$  and blaze angle  $26^\circ 45'$ . The efficiency was 75% at  $5000 \text{ \AA}$  in the first order. The problem of multiple reflection between the grating and tuning mirror  $M_2$  was eliminated by slightly rotating the grating about its normal so that the rulings are not exactly perpendicular to the optical axis of the laser.

In order to satisfy the condition  $d_2 = L_R$  for the minimum laser linewidth,<sup>12</sup> the grating was kept at a distance of  $d_2 = 120$  mm from the centre of the dye cell, ( $d_2$  being the distance from the centre of the dye cell to the centre of the grating).

$$\text{Where } L_R = \frac{\pi \omega^2}{\lambda} \dots (2.11)$$

$2\omega$  is the diameter of the active region at the centre of the dye cell and is approximately equal to the width of the focussed  $N_2$  laser beam which in the present set up is 0.3 mm. Substituting this value for  $\omega$  and  $6000 \text{ \AA}^\circ$  for  $\lambda$  in eq. 2.11 gives  $L_R = 116 \text{ mm}$ .

When  $d_2 \approx L_R$  the laser linewidth<sup>12</sup> is given by the relation

$$\frac{\Delta\lambda}{\lambda} = \frac{\sqrt{2}\lambda}{\pi l(\sin\theta_0 + \sin\phi)} \quad \dots (2.12)$$

Where  $l$  is the width of the illuminated part of the grating,  $\theta_0$  is the angle of incidence and  $\phi$  is the angle of diffraction. Substituting  $\lambda = 6000 \text{ \AA}^\circ$ ,  $l = 25 \text{ mm}$ ,  $\theta_0 = 88^\circ$  and  $\phi = 14.5^\circ$  in equation 2.12 we get the laser linewidth  $\Delta\lambda = 0.05 \text{ \AA}^\circ$ . This shows that the theoretical limit for laser linewidth obtainable with the present set up is  $0.05 \text{ \AA}^\circ$ .

The tuning mirror  $M_2$  was mounted on a precision rotatable mount. This mirror also was aluminium coated on glass substrate of high surface accuracy ( $\sim \frac{\lambda}{10}$ ). The distance between grating and the mirror was 5 cm and thus giving an overall cavity length of 22 cm.

#### 2.34 Alignment

The cross-section of the pumped region of the dye can be roughly adjusted to be circular or square by adjusting

the position of the line focus and dye concentration. The weak fluorescent emission directed to the feedback mirror  $M_1$  is retraced through the active medium. The emerging intense beam is passed through a pinhole of diameter equal to the beam diameter. This beam is allowed to fall on the grating at grazing incidence in such a way that the entire beam falls on the grating. The length of the grating used can be directly observed. The tuning mirror  $M_2$  is thus aligned to retrace the beam through the grating to the active region. This can be easily monitored by observing the expanded beam on the pin hole plate. By adjusting mirror  $M_2$  any convenient section of the expanded beam can be made to fall on the pin hole. Now the zeroth order output beam can be examined for tuned output with the help of a monochromator. A ground glass plate placed at the exit of the monochromator will show a sharp intense line image in the superradiant background. If this line image is not seen a fine adjustment of mirror  $M_1$  will give the tuned output.

### 2.35 Performance Data

The following beam qualities of the present laser set up was measured for  $5 \times 10^{-3}$  M. Rh-5G in Methanol and is given.

Output power	-	15	kW
Divergence	-	2	mrad
Bandwidth	-	0.9	$\text{Å}^{\circ}$
Pulse duration	-	3.5	ns
Conversion efficiency	-	7.5%	

### 2.36 Possible Improvements on the Design

The following improvements can be suggested to the present design for better performance of the system.

1. The grating used in the present set up can be replaced by a holographic grating of greater width (50 mm wide). The feedback efficiency of holographic gratings are higher and the greater width permits the operation of the grating at angle of incidence greater than  $88^{\circ}$ .
2. The flat tuning mirror can be replaced by a curved concave cylindrical mirror to prevent losses due to the vertical beam divergence.
3. The Aluminium Coated (90% reflectivity) mirrors  $M_1$  and  $M_2$  can be replaced by dielectric coated 100% reflecting mirrors so that the efficiency of the system will be increased.

4. A spherical quartz lens can be used in front of the cylindrical lens to reduce the length of the focussed strip of  $N_2$  beam from 2.2 cm to 1 cm thereby wastage of pump power can be avoided.
5. Intracavity etalon can be used to get narrow bandwidth output.

References

1. Lambda Physik Laser Service Chart.
2. F.P. Schafer, Dye lasers, eds. F.P. Schafer.  
(Springer-Verlag, 1977) p. 33.
3. T.W. Hansch, Appl. Opt. 11, 895 (1972).
4. J.E. Lawler, W.A. Fitzsimmons and L. I. Anderson.  
Appl. Opt. 15, 1033 (1976).
5. D.C. Hanna, P.A. Karkkainen and R. Wyatt. Opt.  
Quant. Electr. 7, 115 (1975).
6. S.A. Myers. Opt. Commun. 4, 137 (1971).
7. G. Yamaguchi, F. Endo, S. Murakawa and C. Yamanaka.  
Japan J. Appl. Phys. 7, 179 (1968).
8. F.C. Strome and J.P. Webb. Appl. Opt. 10, 1348 (1971).
9. F.P. Schafer and A. Muller. Opt. Commun. 2, 407  
(1971).
10. L.G. Nair, Appl. Phys. 20, 97 (1979).
11. I. Shoshan, H.N. Danon and U.P. Oppenheim. J. Appl.  
Phys., 48, 4495 (1977).
12. M.G. Littman and H.J. Metcalf. Appl. Opt. 17, 2224  
(1978).

13. I. Shoshan and U.P. Oppenheim, *Opt. Commun.* 25, 375 (1978).
14. H.G. Littman, *Opt. Lett.* 3, 133 (1978).
15. L.G. Nair and K. Dasgupta, *IEEE. J. QE-16*, 111 (1980).
16. U. Ganiel, A. Hardy, G. Neumann and D. Treves, *IEEE. J. QE-11*, 381 (1975).
17. J.J. Wynne, *IEEE J. QE-10*, 125 (1974).
18. H.N. Loiko, Zs. Bor, L. Kozma, B. Racz and I. Ketskemety, *Opt. Commun.* 15, 173 (1975).
19. E.D. Stokes, F.B. Dunning, R.F. Stebbings, G.K. Walters, and R.D. Rundel, *Opt. Commun.* 5, 267 (1972).
20. F. Zaraga, *Appl. Phys.* 4, 37 (1974).
21. O. Hilderbrand, *Opt. Commun.* 10, 310 (1974).
22. I. Itzkan and F.M. Cunningham, *IEEE J. QE-8*, 101 (1972).
23. P. Burlamacchi, R. Coisson, R. Fratesi and D. Pucci, *Appl. Opt.* 16, 1553 (1977).
24. B. Racz, Zs. Bor, S. Szatmari and G. Szabo, *Opt. Commun.* 36, 399 (1981).

CHAPTER III

PARAMETRIC MEASUREMENTS OF THE DYE LASER

ABSTRACT

The general properties of organic dyes as a laser active medium is discussed. The basic parameters such as power output, conversion efficiency, pulse duration, divergence, bandwidth, polarization and tunability of the fabricated dye laser are studied in detail. The output power is found to vary linearly with input pump power. The conversion efficiency decreases with bandwidth. A 3 ns dye laser pulse is obtained with Rh-6G in methanol. A dependence of beam divergence on the distance between feedback mirror and centre of the dye cell is established. It is found that the feedback mirror had to be placed atleast 3 cm away from the centre of the dye cell to get diffraction limited beam divergence. The bandwidth is studied as a function of angle of incidence on the grating as well as beam divergence. The polarization studies on the output beam have shown that the  $10^\circ$  wedge angle of the dye cell windows with respect to the laser axis increases the degree of polarization of the beam. However, no polarization competition effect is observed. The tunability range and the emission peaks for the dyes Rh-6G, Rh-B, Safranin T, C 120, and dimethyl POPOP are studied.

### 3.10 Introduction

Numerous approaches to obtain tunable narrow band and high power emission from organic dye lasers have been reported. A coarse selection of the laser wavelength is possible by a suitable selection of the dye, its concentration,<sup>1</sup> the solvent<sup>3-6</sup> and the cell length.<sup>1</sup> But narrow band wavelength tuning can be achieved only by using a wavelength selective resonator. Soffer and McFarland<sup>7</sup> constructed the first wavelength selective resonator with a plane grating in place of one of the mirrors and obtained a spectral width of 0.6 Å. The spectral narrowing can also be achieved by using one or more prisms in the laser cavity.<sup>8-10</sup> A spectral width of 0.1 Å has been achieved using six prisms by Schafer et al.<sup>11</sup> The use of Fabry-Perot etalon<sup>12,13</sup> within the cavity gives much smaller bandwidths. Hansch<sup>12</sup> could obtain a spectral width of 0.004 Å using a combination of a Fabry-Perot etalon, a beam expanding telescope and a grating. More recently Shoshan<sup>14</sup> has described a method employing grating at grazing incidence and obtained a spectral width of 0.03 Å. Owing to its simplicity and satisfactory performance the design of Shoshan is now widely accepted by many investigators<sup>15,16</sup> for N<sub>2</sub> laser pumped dye lasers. Several other methods of wavelength selection making use of polarization with a birefringent filter in the cavity,<sup>17</sup> rotatory dispersion of z-cut

quartz crystal,<sup>18</sup> the Faraday rotation in the vicinity of an atomic absorption line,<sup>19</sup> pressure scanning,<sup>20</sup> wavelength selective distributed feedback resonators and selective reflection at glass atomic vapour interface<sup>23</sup> have been reported.

The simultaneous efforts made to improve the conversion efficiency of dye lasers show remarkable progress even though the overall efficiency of dye lasers is deplorably bad since the pump laser ( $N_2$ ) efficiency is very low. Most of the reported results are showing a conversion efficiency in the range 2 to 11% depending upon the design and bandwidth. Itzkan et al.<sup>24</sup> obtained a conversion efficiency of 25% by using an oscillator-amplifier dye laser system. It was also shown by Lawler et al.<sup>25</sup> that the conversion efficiency can be greatly improved if the temporal distribution of the  $N_2$  pump pulse is adjusted so that the single cell first acts as an oscillator and then as an amplifier. A substantial enhancement of conversion efficiency is possible by using mixed dye systems.<sup>26-28</sup>

### 3.20 Properties of Laser Dyes

The characteristics of the dye laser output beam depends on the physical and chemical properties of the active

medium (the organic dye) as well as on the parameters of the cavity. The process of light absorption and the kinetics and reactions of the excited dye molecule determine the suitability of the dye as a laser active medium. These properties of the dye molecules and also the oscillation conditions are discussed below.

### 3.21 Light Absorption

Organic dyes which contain an extended system of conjugated bonds are characterised by a strong absorption band in the visible region of the electromagnetic spectrum. The energy level diagram of a typical dye molecule is shown in Fig. 3.1. The long wavelength absorption band of dyes is attributed to the transition from the electronic ground state  $S_0$  to the first excited singlet state  $S_1$ . When pumped, dye molecules are raised to the lowest excited singlet state  $S_1$ , either directly or via some higher singlet state which relaxes quickly to  $S_1$ . Lasing involves the return to the ground state  $S_0$  by stimulated emission of a photon.

The long wavelength limit of absorption band is closely related to the thermal stability of the dye molecule. A dye absorbing in the near-infrared has a low lying excited singlet state and a slightly lower metastable triplet state.

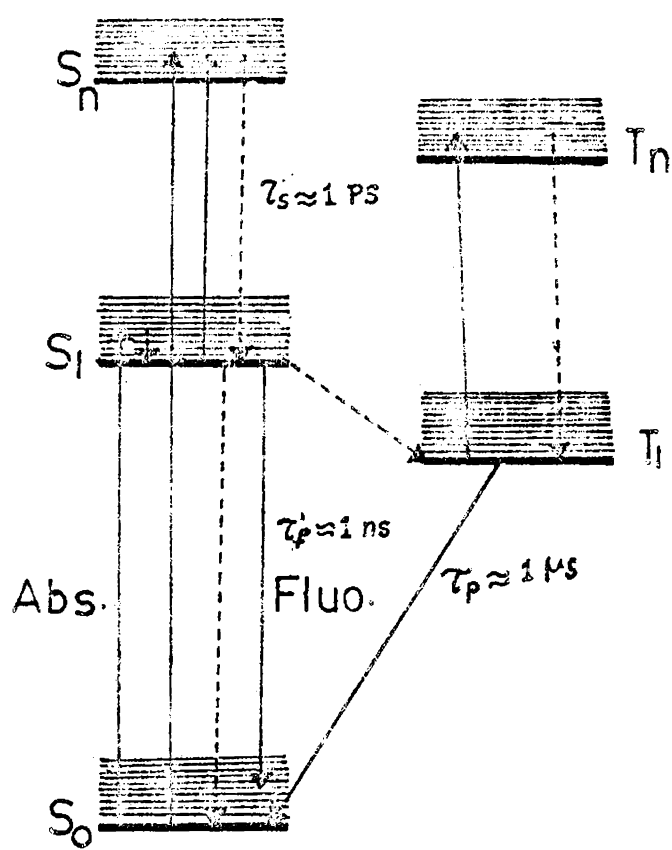


Fig.3.1. Schematic energy level diagram for a dye molecule

The triplet state has two unpaired electrons. Most of the dye molecules that reach this highly reactive state by thermal excitation will react with solvent molecules, impurities or other dye molecules to yield decomposition products. Hence the thermal instability of dye molecules puts an upper limit to the long wavelength absorption and hence to long wavelength lasing. The short wavelength limit of dye laser is given by the absorption of dyes containing only two conjugated double bonds. Such a dye has absorption bands at wavelengths of about 220 nm. Since the energy absorbed at this wavelength is higher than the energy of any bond in the molecule, photochemical decomposition effectively competes with radiative deactivation.

A peculiarity of the spectra of organic dyes is the width of the absorption bands. In the case of a large dye molecule, many vibrational modes are coupled to the electronic transitions. After the electronic excitation has occurred, there is a change in the bond length due to the change in electron density. As a result, the neighbouring atoms constituting the bond will start to oscillate around the new position with an amplitude  $r^* - r$  where  $r^*$  is the new bond length before electronic excitation. A molecular skeletal vibration is excited in this way. Further more, collision and electrostatic perturbations caused by the surrounding solvent molecules

broaden the individual lines of such vibrational series. The rotationally excited sublevels further broadens the spectra and a quasi continuum of states superimposed on every electronic level is obtained. The same is true for the fluorescence emission also.

The organic dye spectra will be modified due to the effects of temperature, concentration and acid-base equilibria with the solvent. If the temperature of a dye solution is increased, higher vibrational levels of the ground state are populated according to a Boltzmann distribution, and the transitions from these levels to higher sublevels of first excited singlet state broadens the spectra. But this can be avoided by cooling the dye solution to the glass point. The formation of dimers and higher aggregates makes the absorption spectra shifted to shorter wavelengths with an additional weaker band at the long wavelength side of the monomer band. The equilibrium between monomers and dimers shifts to the side of the latter with increasing dye concentration and with decreasing temperature. Moreover, dimer formation is more pronounced in solution of high dielectric constant; notably water. These dimers not only absorb a part of the pump light but also the monomer emission. The attractive dispersion forces between the large dye molecules tend to bring the dye molecules together in a position with the planes of the molecules

parallel, where the interaction energy is highest; while the high dielectric constant of the solvent reduces the Coulombic repulsion between the identically charged molecules. The situation favours the aggregation of dye molecules. The dimer formation can be avoided by using a less polar solvent like alcohol or by adding a detergent to the aqueous dye solution, which then forms micelles that contain one dye molecule each. The acid-base equilibria with the solvent also causes spectral shifts since many dyes can exist as cationic, neutral and anionic molecules depending on the PH of the solution.

### 3.22 Laser Emission and Quantum Yield of Fluorescence

The dye molecules excited to higher levels in the singlet manifold will relax within picoseconds to the lowest vibronic level of  $S_1$ . The transition  $S_1 \rightarrow S_0$  causes the stimulated laser emission in dye lasers. But this light emission has competition from several other processes, mainly from the nonradiative conversion to the ground state ( $S_1 \rightarrow S_0$ ) and from the intersystem crossing to the triplet manifold, ( $S_1 \rightarrow T_1$ ). In addition, the  $S \rightarrow S$  absorption and  $T \rightarrow T$  absorption of the pump light or laser emission reduces the efficiency of the laser system. The presence of a quenching agent in the dye solution also reduces the fluorescence efficiency.

The quantum yield of fluorescence,  $\Phi_f$  is defined as the ratio of radiative and nonradiative transition rates and is given by

$$\Phi_f = \frac{1/\tau_{rf}}{1/\tau_{rf} + K_{ST} + K_{SG} + K_Q [Q]} \quad \text{-----(31)}$$

where  $\tau_{rf}$  is the radiative life time,  $K_{ST}$  is the rate constant for the processes  $S_1 \rightarrow T_1$ ,  $K_{SG}$  the rate constant for internal conversion and  $K_Q$  the rate constant for fluorescence quenching due to  $[Q]$  (the concentration of quencher) and is equal to the diffusion controlled binolecular rate constant.

### 3.23 Oscillation Condition

A dye laser consists of a cuvette of length  $L$  (cm) with dye solution of concentration  $n$  ( $\text{cm}^{-3}$ ) and of two parallel end windows each of reflectivity  $R$  for the laser resonator. With  $n_1$  molecules/ $\text{cm}^3$  excited to the first singlet state, the dye laser will start oscillating at a wave number  $\bar{\nu}$ , if the overall gain

$$\exp[-\sigma_a(\bar{\nu})n_0 L] R \exp[+\sigma_f(\bar{\nu})n_1 L] \geq 1$$

where  $\sigma_a(\bar{\nu})$  and  $\sigma_f(\bar{\nu})$  are the cross-sections for absorption and stimulated fluorescence at  $\bar{\nu}$ , respectively and  $n_0$  is the ground state population.

The above expression for gain can be written in the form

$$\frac{S/n + \sigma_a(\bar{\nu})}{\sigma_f(\bar{\nu}) + \sigma_a(\bar{\nu})} \leq \mathcal{V}(\bar{\nu}) \quad \dots (3.2)$$

Where  $S = \frac{1}{L} \ln \frac{1}{R}$  and  $\mathcal{V}(\bar{\nu}) = \frac{n}{n_1}$

From the above expression, since  $\mathcal{V}(\bar{\nu})$  is the minimum fraction of molecules that must be raised to the first singlet state to reach the threshold level for oscillation, it is evident that the peak laser wavelengths can be changed by changing the concentration of dye solution ( $n$ ), cell length ( $L$ ) or  $Q$  of the resonating cavity ( $R$ ).

The absorbed power density  $W$  necessary to maintain the fraction  $\mathcal{V}$  of the molecular concentration  $n$  in the excited state is given by

$$W = \mathcal{V} n h c_0 \bar{\nu}_p / \tau_f \quad \dots (3.3)$$

and if the incident radiation is completely absorbed in the dye sample, the power flux

$$P = \frac{W}{n \sigma} = \mathcal{V} h c_0 \bar{\nu}_p / \tau_f \sigma \quad \dots (3.4)$$

Where  $\bar{\nu}_p$  is the wave number of the absorbed pump radiation

and  $\sigma$  its cross section. If the radiation is not completely absorbed

$$W = W_{in} \sigma_p nL \quad \dots (3.5)$$

Then the threshold incident power flux is

$$P_{in} = \gamma_{hc} \gamma_p / \tau_f \sigma_p \quad \dots (3.6)$$

### 3.30 Basic parameters of a dye laser

For the optimization of the performance of a dye laser system a parametric study of the system is essential. The basic parameters of a dye laser system are power output, conversion efficiency, pulse duration, divergence, bandwidth, polarization and tunability. These beam qualities of the dye laser system fabricated for the present investigation and their dependence on the system parameters are illustrated in this section.

### 3.31 Power output and conversion efficiency

The power measurements were carried out using a SCIENTECH 1<sup>st</sup> disc calorimeter. The experimental arrangement is shown in Fig. 3.2. The N<sub>2</sub> laser power was monitored by a

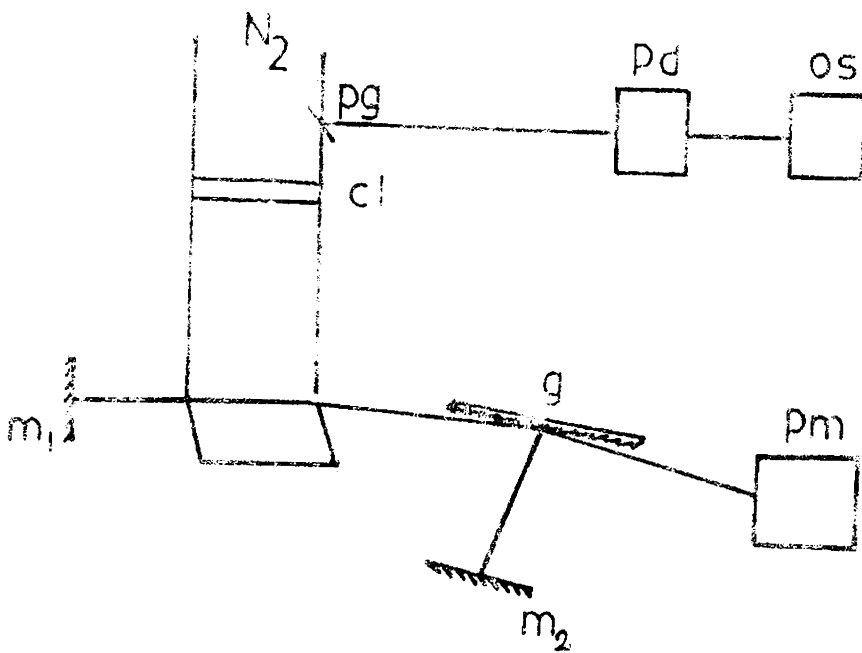


**Fig.3.2. The experimental arrangement for power measurements of the Dye laser. (Pm) power meter, (Pd) photo diode, (os) Oscilloscope, (pg) Plane glass plate.**

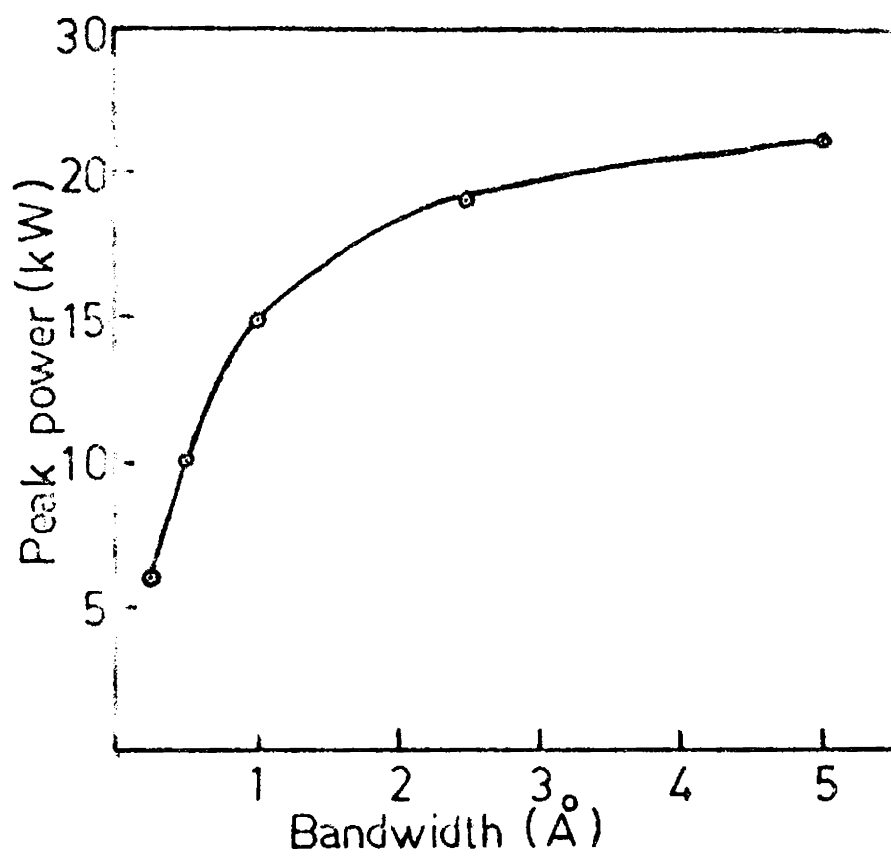


**Fig.3.3(A). Dye laser peak power versus bandwidth.**

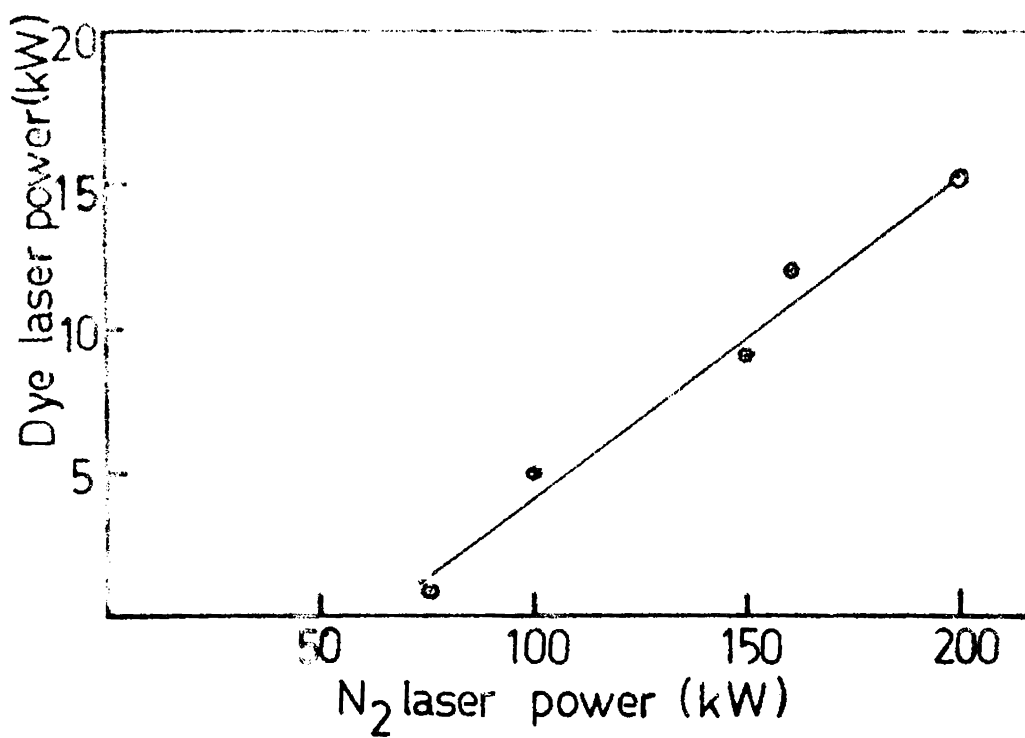


**Fig.3.3(B).** Dye laser power versus N<sub>2</sub> laser power for a  $5 \times 10^{-3}$  M solution of Rh 6G in methanol.

fast pin type photodiode (HP<sub>2</sub>-4207 Hewlette Packard) and a TEKTRONIX storage oscilloscope (model 456). The narrow band dye laser output ( $\Delta\lambda = 1 \text{ \AA}$ ) is directed to the calorimeter and the energy for 600 pulses is noted. The pulse repetition rate was measured with a Geiger counting system.

The pulse duration obtained from the oscilloscope is used to calculate the peak power output  $p = \frac{\text{Energy/Pulse}}{\text{Pulse duration}}$ . The maximum obtained peak power was 15 kW for a  $5 \times 10^{-3} \text{ M}$  solution of Rh-6G in methanol at a pump power of 200 kW. The back ground superradiance which is super imposed on the narrow band laser beam is taken into account during all power measurements by providing a graphical correction on the observed values. When the bandwidth was increased to  $5 \text{ \AA}$  the output power obtained was 21 kW. This shows a conversion efficiency of 10.5%. The variation of output power with bandwidth is shown in Fig. 3.3. It can be seen from the plot that the conversion efficiency drops to 3% when the bandwidth is reduced to  $0.25 \text{ \AA}$ . The feedback efficiency of the grating used was very low for narrow band operation and hence the conversion efficiency too was very small.

The variation of dye laser power with pump power was studied by changing the  $\text{N}_2$  laser power from 75 kW to 200 kW. The corresponding dye laser output power for a  $5 \times 10^{-3} \text{ M}$  solution of Rh-6G in methanol at a bandwidth of  $1 \text{ \AA}$  was

measured. Fig. 3.3 shows the plot of the dependence of dye laser power on  $N_2$  laser power. Within the range studied it is observed that the dye laser output increases linearly with pump laser power.

### 3.32 Pulse Characteristics

The pulse shape and duration was traced using a fast photodiode and a Tektronix storage oscilloscope. The pulse measuring circuit is shown in Fig. 3.4. The pulse shape and duration of the  $N_2$  laser as well as the dye laser traced using the above circuit are shown in plates 1 and 2. The  $N_2$  pulse duration is 8 nsec (FWHM) and the dye laser duration is 3 nsec (FWHM). The  $N_2$  pulse shows a shoulder pulse which is due to the back reflection from the rear mirror of the  $N_2$  Laser cavity. The dye laser pulse also shows the same shoulder pulse indicating that the dye laser pulse closely follows the pumping pulse above the threshold level.

### 3.33 Divergence

The divergence measurements of the laser beam are carried out by measuring the far field intensity distribution across the beam using a photodiode and oscilloscope. The experimental arrangement is illustrated in Fig. 3.5. The

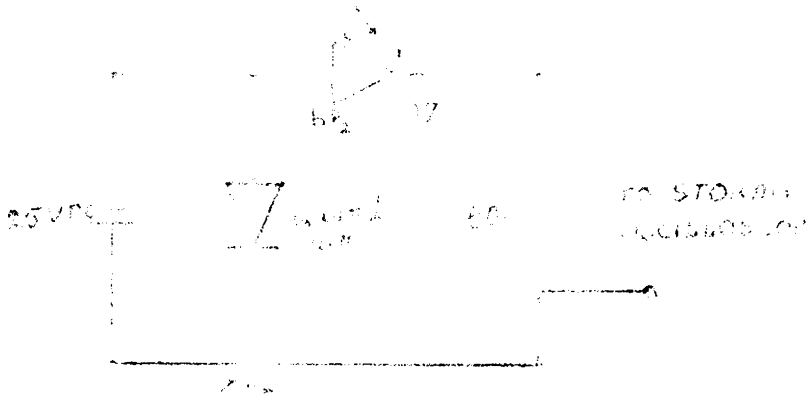


**Fig.3.4. Pulse measuring circuit.**

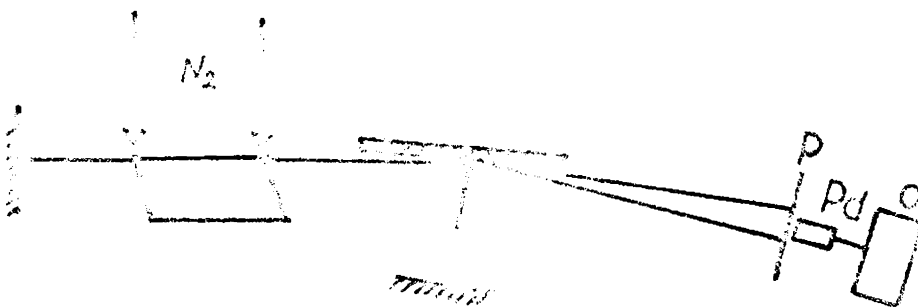


**Fig. 3.5. Experimental arrangement for divergence measurements.**

photodiode masked with a pinhole was moved across the beam at about 5 meters away from the dye cell. The pulse heights at different points across the beam were noted. The plot of intensity (pulse height) versus distance across the beam given in Fig. 3.6 shows that the laser beam has approximately a gaussian profile. The gaussian profile of the laser beam at distances of 6 and 5 meters away from the dye cell are used to calculate the semi angular divergence of the beam. The minimum divergence obtained is 1.2 mrad.

It is observed that the distance from the centre of the dye cell to the feedback mirror close to the cell has a drastic dependence on the divergence of the laser beam. The feedback mirror position was varied from 3 to 10 cm from the centre of the dye cell and the divergence of the output beam was measured. The divergence of 8 mrad when the mirror was at a distance of 3 cm was reduced to 1.2 mrad when the distance was 8 cm. A further increase in distance did not show any reduction in divergence. The plot of feedback mirror distance versus semi angular divergence is shown in Fig. 3.7. An increase in angular divergence over the diffraction limit increases the bandwidth also, since the effective slit size of the active region at the centre of the dye cell increases. Hence in order to get a diffraction limited divergence and thereby a narrow bandwidth the feedback mirror had to be placed at a distance of 8 cm away from the centre of the dye cell in the present set up.

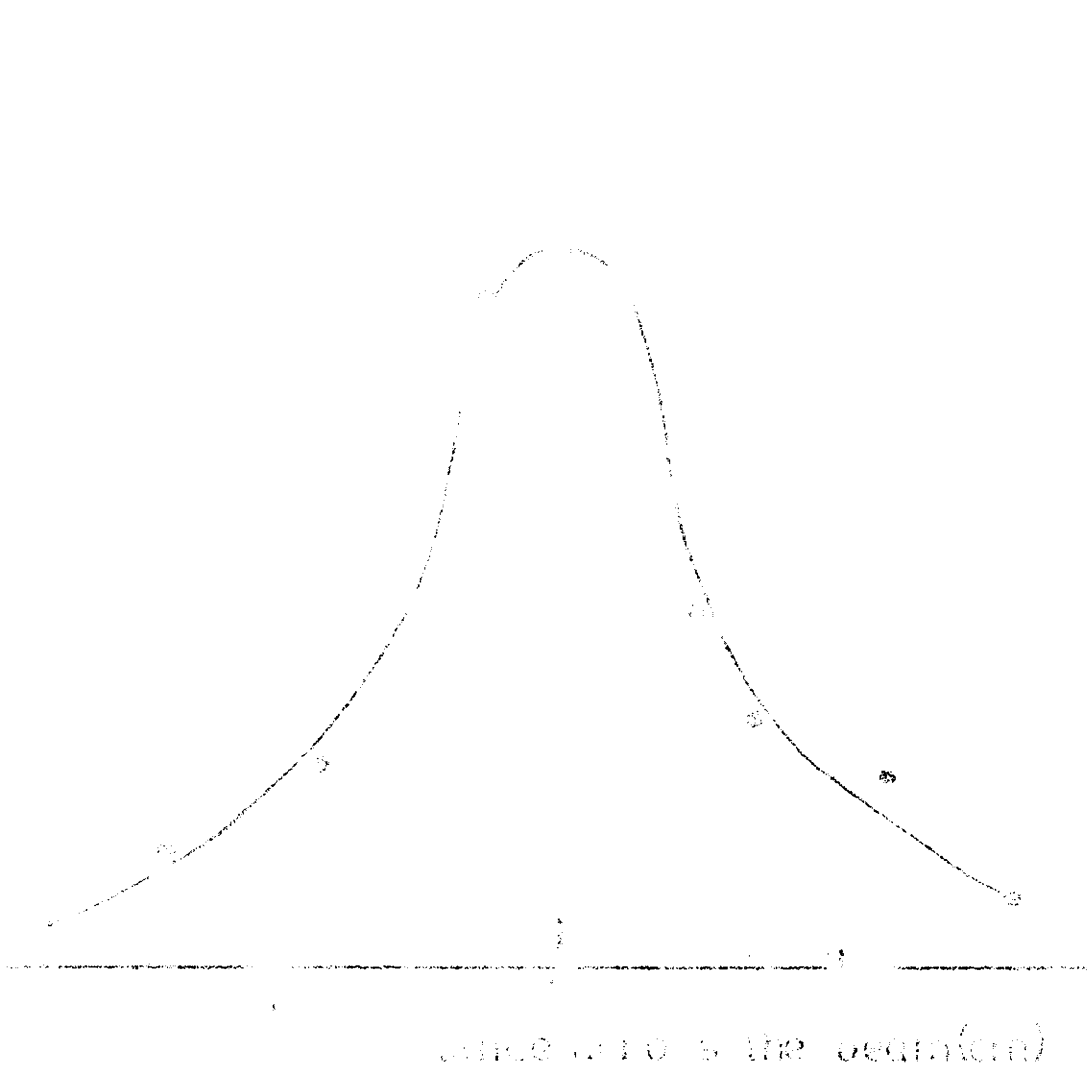


**Fig.3.6. Spatial intensity profile of the dye laser output.**

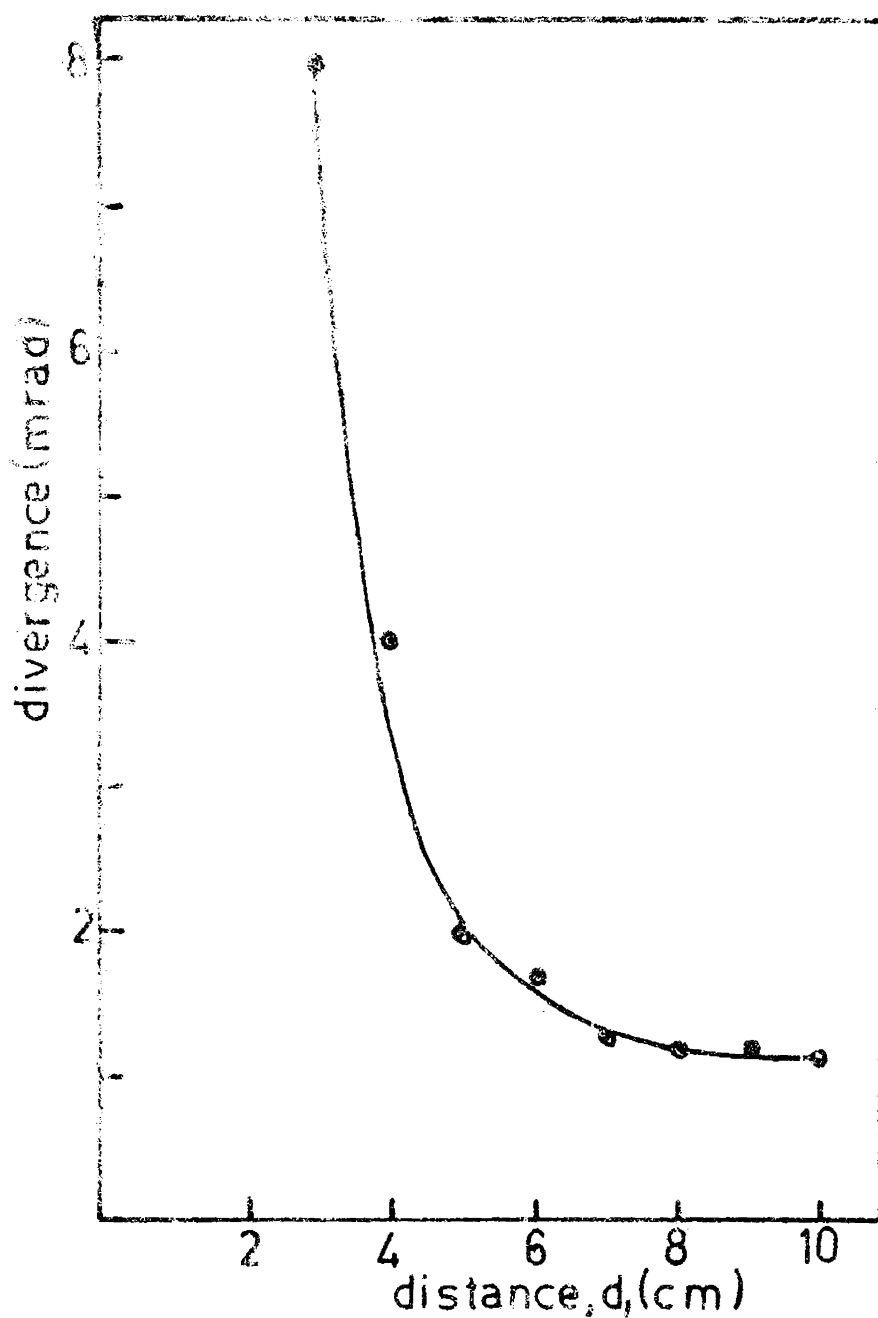


**Fig.3.7. Dependence of divergence on the feedback mirror position with respect to the center of the dye cell.**

3.34 Bandwidth

A Jarrell-Ash 0.5 meter scanning monochromator with a spectral resolution of  $0.15 \text{ \AA}$  was used, along with an EMI 9604 QB photo multiplier and an omniscrite chart recorder, for the measurement of bandwidth of the laser beam. Since the minimum obtained bandwidth was  $0.25 \text{ \AA}$ , the use of such a monochromator for the bandwidth measurement is justified. The arrangement used is shown in Fig. 3.8. Fig. 3.9 is the chart recorder trace of the output spectrum for a  $5 \times 10^{-3} \text{ M}$  Rh-6G solution in methanol and with the feedback mirror at a distance of 7 cm away from the centre of the dye cell. It shows a bandwidth of  $0.25 \text{ \AA}$ .

Attempts made to achieve still smaller bandwidths obtainable with the present geometry of the dye laser were unsuccessful and the following difficulties are attributed to this. First of all the feedback efficiency of the grating used was insufficient to get amplification at very large angle of incidence. The grating could be used only upto an angle of incidence of  $88^\circ$ . Moreover it was observed that the feedback mirror position, which had a drastic effect on the divergence of the laser beam, also influenced the bandwidth. The variation of bandwidth with angle of incidence of the grating for three different positions of the feedback mirror is shown

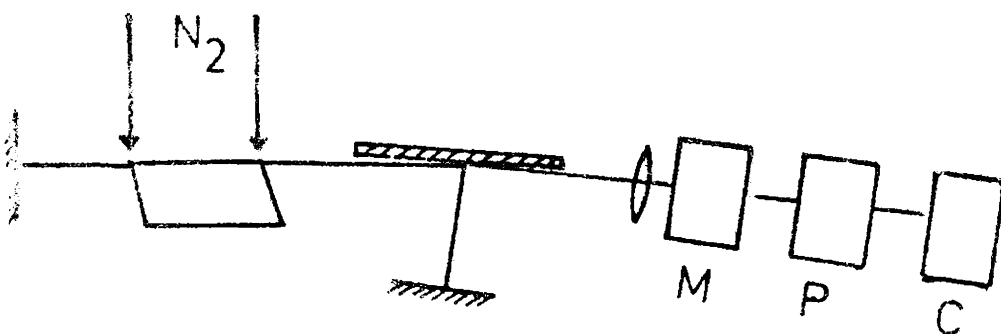


**Fig.3.8. Experimental arrangement for bandwidth measurements. (M) Monochromator, (P) Photomultiplier, (C) Chart recorder.**

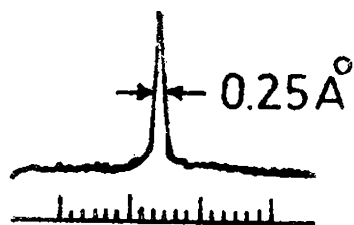


**Fig.3.9. Chart recorder trace of the dye laser output spectrum with feedback mirror 7 cm away from the center of the dye cell. (1 cm = 1  $\text{\AA}$ ).**

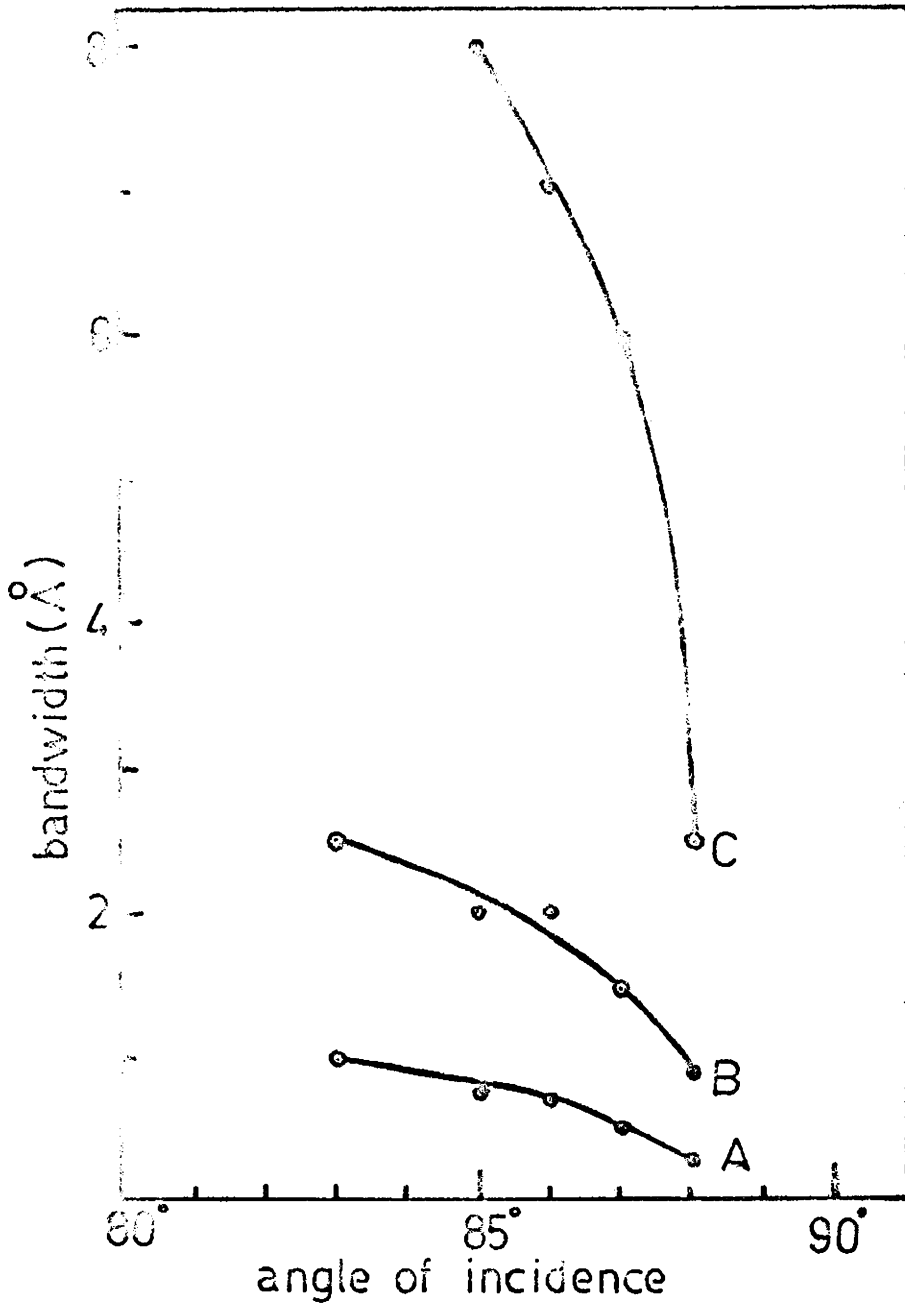


**Fig.3.10. Bandwidth versus angle of incidence on the grating for different feedback mirror position. (A) Feedback mirror at a distance of 7 cm, (B) 5 cm, and (C) 3.5 cm away from the centre of the dye cell.**

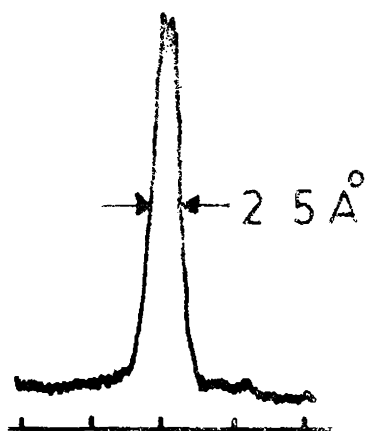


**Fig.3.11. Chart recorder trace of dye laser output spectrum for  $83^\circ$  angle of incidence and feedback mirror distance of 5 cm from the center of the dye cell. ( 1 cm =  $5 \text{ \AA}$  ).**

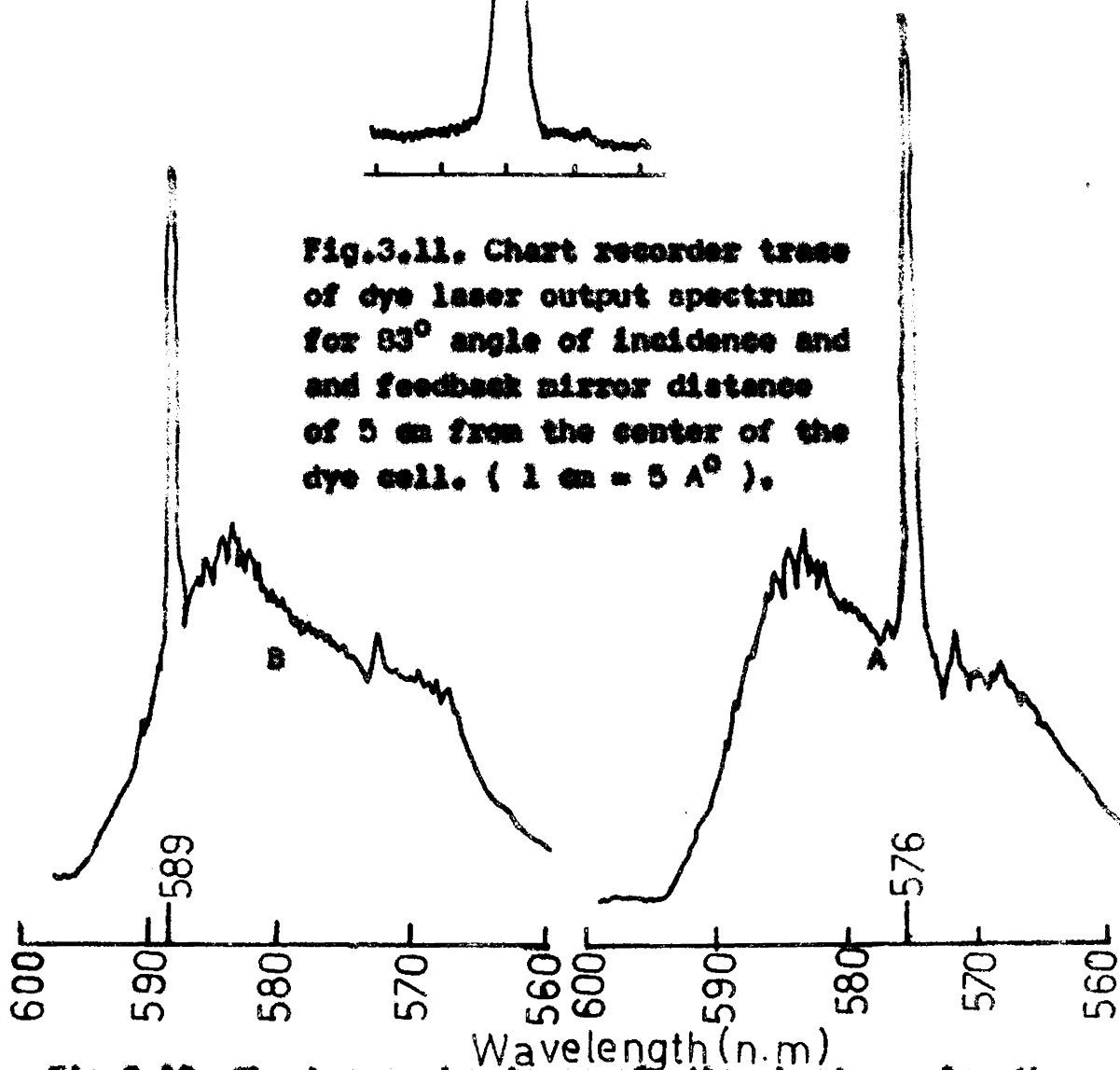


**Fig.3.12. Chart recorder trace of the short wavelength lasing(A) and long wavelength lasing (B) of a  $5 \times 10^{-3}$  M solution of Rh 6G in methanol.**

in Fig. 3.10. Fig. 3.11 is the recorded trace showing  $\Delta\lambda = 2.5 \text{ \AA}^\circ$  at  $83^\circ$  angle of incidence and feedback mirror 5 cm away from the cell. It can be seen that when the beam divergence is a maximum the bandwidth is substantially high. The minimum bandwidth obtained for  $88^\circ$  angle of incidence of the grating was  $2.5 \text{ \AA}^\circ$  when the divergence was 7 mrad whereas the minimum bandwidth of  $0.25 \text{ \AA}^\circ$  was obtained when the beam divergence was 1.75 mrad. The diffraction limited beam divergence of 1.2 mrad is obtained only when the feedback mirror was 3 cm away from the dye cell. At this position the efficiency of the cavity was very low to get tuned output. These difficulties did not permit to reduce the linewidth less than  $0.25 \text{ \AA}^\circ$ .

### 3.35 Polarization effect due to the $10^\circ$ Wedge Angle of the Dye Cell

The polarization of the dye laser beam is determined mainly by the polarization of the exciting beam, the relative orientation of the transition moments in the dye molecules for the pumping and laser transitions and the rotational diffusion-relaxation time. Only very few experimental investigations have been reported in this field.<sup>29-31</sup> Since the polarization of dye laser beam can be manipulated by introducing into the resonator polarizing elements like Brewster windows,

most of the investigations reported were taken with such polarizing elements in the cavity. For the present investigations on polarization of the dye laser beam, no intracavity polarizing elements were used. But the  $10^\circ$  wedge angle of the dye cell windows with the laser axis, a common design aspect employed in  $N_2$  Laser pumped dye lasers, can act as a partial polarizing element. Since the zeroth order reflection from the grating is taken as the output, this reflection also can introduce some polarization. An attempt is made to investigate the effect of the wedge angle and the reflection on the grating on the polarization of the output beam. The degree of polarization of the dye laser beam for a given pump polarization has also been investigated.

The narrow band dye laser output ( $\Delta\lambda = 0.8 \text{ \AA}$ ) at the emission peak of the dye was directed to the monochromator to eliminate the superradiant background. The intensity  $I_p$  and  $I_s$  of the beam for the two orthogonal polarization is measured with a photomultiplier and chart recorder by inserting the parallel and perpendicular polarization filters in front of the entrance slit of the monochromator. The tilt of the dye cell was  $10^\circ$  and the angle of incidence of the grating in the laser cavity was  $88^\circ$ . The degree of polarization  $P = \frac{I_p - I_s}{I_p + I_s}$  is calculated.

In a similar manner the degree of polarization of the superradiant dye laser beam (without feedback mirror and with  $0^\circ$  tilt for the dye cell) is also calculated. In this case also the intensities were measured at the peak of the emission spectrum. The  $N_2$  Laser beam was monitored by a photodiode and oscilloscope. The degree of polarization of the pumping laser beam, the tuned and superradiant dye laser beams for  $5 \times 10^{-3} M$  Rh-6G and  $2.5 \times 10^{-3} M$  Rh-B and that for tuned outputs of  $2 \times 10^{-3} M$  C 120  $2 \times 10^{-3} M$  Dimethyl POPOP and dye mixtures Rh-6G + C 120 and Rh-6G + Rh-B are given in Table 2. The solvent used for all the dyes was methanol except for Dimethyl POPOP which was dissolved in benzene.

The degree of polarization for the superradiant beam is less than that for the tuned laser beam. The difference in the degree of polarization is due to the polarization introduced by the tilt of the dye cell and the reflection at the grating. A prior test on the cavity grating with a randomly polarized He-He laser showed that at  $83^\circ$  angle of incidence it introduces a 2% polarization. But the observed difference in the degree of polarization of the tuned and superradiant beam is greater than this value. Hence it can be concluded that the excess degree of polarization is due to the tilt of the dye cell which is the only other polarizing element in the cavity. The loss introduced for one polarizati

Table 2

Laser	Concentration M/l	Solvent	Degree of Polarization P
N <sub>2</sub>	--	--	+ 0.33
Superradiant Rh-6G	5 X 10 <sup>-3</sup>	Methanol	- 0.27
Tuned Rh-6G	5 X 10 <sup>-3</sup>	Methanol	- 0.31
Superradiant Rh-B	2.5 X 10 <sup>-3</sup>	Methanol	- 0.27
Tuned Rh-B	2.5 X 10 <sup>-3</sup>	Methanol	- 0.33
Tuned C 120	2 X 10 <sup>-3</sup>	Methanol	+ 0.33
Tuned POPOP	2 X 10 <sup>-3</sup>	Benzene	+ 0.65
Tuned Rh-6G + C 120	2 X 10 <sup>-3</sup> (Rh-6G), 2 X 10 <sup>-3</sup> (C 120)	Methanol	- 0.03
Tuned Rh-6G + Rh-B	5 X 10 <sup>-3</sup> (Rh-6G), 5 X 10 <sup>-3</sup> (Rh-B)	Methanol	- 0.13

by the tilt and grating is not enough to drive the oscillator below threshold in that polarization. But by introducing an extra polarizing element in the cavity a sufficient loss to one polarization can be given and therefore it is possible to get polarization competition effect between the two orthogonal polarizations as shown by Dugan et al.<sup>30</sup>

It can be seen from Table 2 that the polarization of Rh-6G and Rh-B is negative and that for C 120 and dimethyl POPOP is positive. McFarland<sup>29</sup> observed a negative polarization for Rh-6G when pumped by the second harmonic of Ruby Laser and positive polarization when pumped with visible radiation.

### 3.36 Tunability

A unique feature of dye laser is the relatively wide spectral range of a single dye at a particular concentration over which tuned output can be obtained. Most of the dyes can be tuned over a range of approximately 35 nm. Even this range can be extended to about 60 nm by changing the concentration of the dye as in the case of DFFC bromide.<sup>32</sup> The emission range of the dyes can be shifted not only by changing the concentration but also by the use of different solvents.<sup>33</sup> A shift of 26 nm of the dye laser emission with changing solvents in the case of a  $10^{-4}$  M solution of the dye

1,1-diethyl- $\beta$ -nitro-4,4-dicyanocyanine tetrafluoroborate is reported.<sup>33</sup>

For the present investigations the dyes 1,4-Di-[2-(4-dimethyl-5-phenyloxazolyl)] - benzene (Dimethyl POPOP) obtained from Koch-Light Laboratories Ltd. England, C 120 from Lambda Physik Germany, Rh-6G from Loba India, Rh-B from E. Merck India and Safranin T from Biedel Germany were used without any further purification.

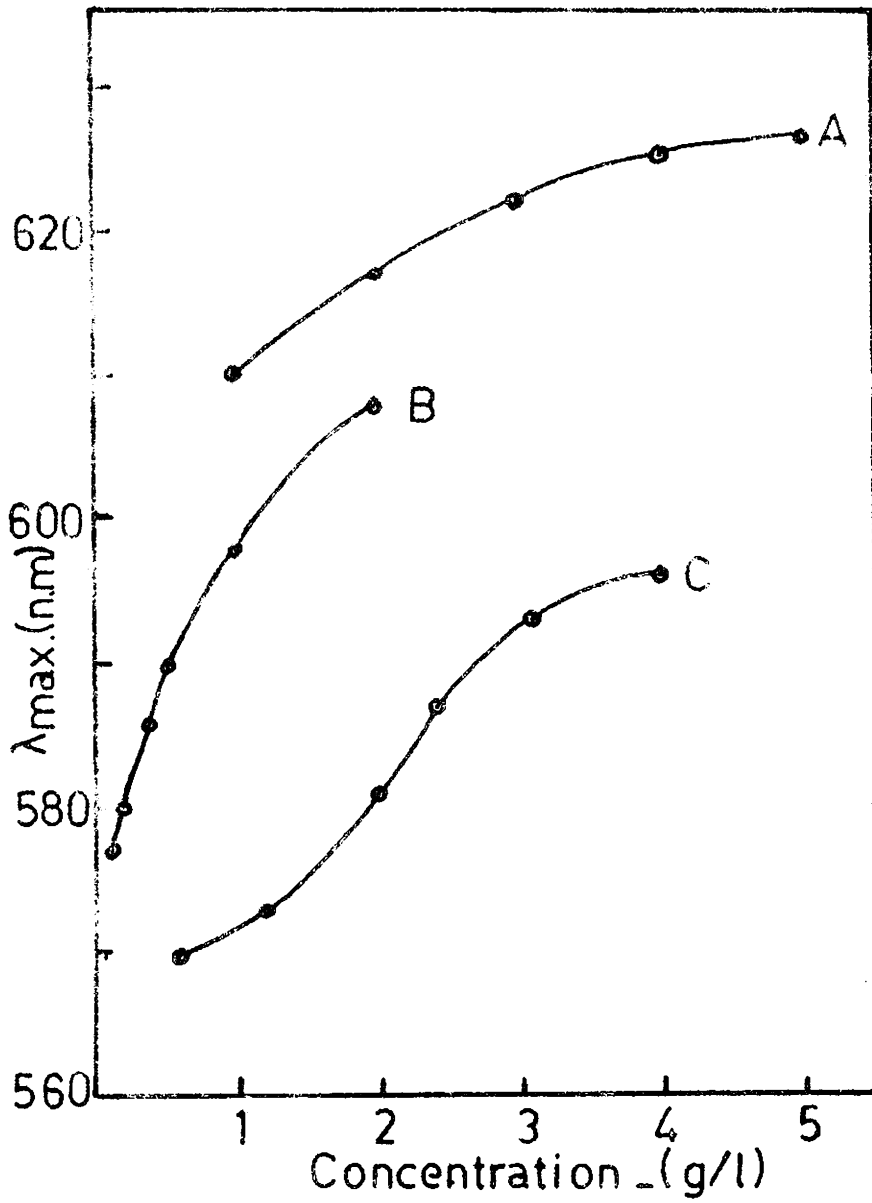
For a fixed concentration the tunability range of the dyes was determined by recording the output spectrum with the monochromator, photomultiplier and chart recorder. The tuning mirror was positioned at the short and long wavelength region of the emission spectrum where lasing section could be obtained. Fig. 3.12 show the short and long wavelength lasing of a  $5 \times 10^{-3}$  M Rh-6G solution in methanol. From the figures it is clear that the tuning range for  $5 \times 10^{-3}$  M Rh-6G methanol is 13 nm. The tuning range for the different dyes, their concentrations and solvent along with emission peaks are given in Table 3. The tuning range of Safranin T is given when it was lased by energy transfer from Rh-6G. The dye was not lasing by itself with  $N_2$  laser pumping. The tuning range obtained for most of the dyes are smaller than that reported earlier. The limitation of pumping power ( $\sim 150$  kW) and the some what small cavity Q can account for the reduced range observed.

Table 3

Dyes	Solvent	Concentration M/l	Tuning range	$\lambda_{\max}$ nm
Rhodamin 6G	Methanol	$5 \times 10^{-3}$	575 - 589	584
Rhodamin B	Methanol	$5 \times 10^{-3}$	612 - 627	621
Safranin T	Methanol	$3 \times 10^{-3}$	585 - 608	598
Coumarin 120	Methanol	$2 \times 10^{-3}$	435 - 445	440
Dimethyl POPOP	Benzene	$2 \times 10^{-3}$	426 - 435	431

Table 4

Dyes	Solvent	Concentration range M/l	Tuning range nm
Rhodamin 6G	Methanol	$1.25 \times 10^{-3}$ -- $8 \times 10^{-3}$	568 - 602
Rhodamin B	Methanol	$2 \times 10^{-3}$ -- $10^{-2}$	605 - 631
Safranin T	Methanol	$0.3 \times 10^{-3}$ -- $6 \times 10^{-3}$	575 - 611
Coumarin 120	Methanol	$1 \times 10^{-3}$ -- $3 \times 10^{-3}$	425 - 450
Dimethyl POPOP	Benzene	$1 \times 10^{-3}$ -- $2 \times 10^{-3}$	416 - 439



**Fig.3.13. Peak emission wavelength versus concentration for the dyes Rh B (A), Safranin T (B) and Rh 6G (C).**

But an enhanced tuning range for a single dye can be obtained by changing the concentration. The concentration of the dyes was changed from the lowest to the highest possible value where lasing action could be obtained. The tuning range obtained is from the short wavelength lasing at the lowest concentration to the long wavelength lasing at the highest concentration. The tuning range, concentration and peak emission at each concentration is given in Table 4. Here again because of the reasons stated above the tuning range obtained was smaller than the previously reported values. It can be seen that the emission peak wavelength changes with concentration. Fig. 3.13 shows the plot of  $\lambda_{\text{max}}$  versus concentration for the dyes Rh-6G, Rh-B and Safranin T.

References

1. G.I. Farmer, B.G. Luth and L.M. Taylor. Appl. Opt., 8, 363 (1969).
2. T. Urisu and K. Kajiyama. J. Appl. Phys., 47, 3559 (1976).
3. F.P. Schafer, W. Schmidt and J. Volkmann. Appl. Phys. Letters, 9, 306 (1966).
4. J.A. Halstead and R.R. Reeves. Opt. Commun. 27, 273 (1978).
5. T. Govindanunni and B.M. Sivaram. Opt. Commun. 32, 425 (1980).
6. M.H. Wong, R.A. Heckman and Z.A. Schelly. J. Phys. Chem. 77, 1317 (1973).
7. B.H. Soffer and B.B. McFarland, Appl. Phys. Letters, 10, 266 (1967).
8. G. Yamaguchi, F. Endo, S. Murakawa, S. Okamura and C. Yamanaka. Japan J. Appl. Phys., 7, 179 (1968).
9. F.C. Strome and J.P. Webb. Appl. Opt., 10, 1348 (1971).
10. F.P. Schafer and H. Muller. Opt. Commun. 2, 407 (1971).

11. F.P. Schafer, Dye Lasers, eds. F.P. Schafer (Springer - Verlag, 1977) p. 70.
12. T.W. Hansch. Appl. Opt., 11, 395 (1972).
13. D.J. Bradley and A.J.F. Durrant. Phys. Lett. 27 A, 73 (1968).
14. I. Shoshan, N.N. Danon and U.P. Oppenheim. J. Appl. Phys., 48, 4495 (1977).
15. H.G. Littman and M.J. Metcalf. Appl. Opt. 17, 2224 (1978).
16. L.G. Nair and K. Dasgupta I. E.E.C. J. QE-16, 111 (1978).
17. B. S oep. Opt. Commun, 1, 433 (1970).
18. D. Kato and T. Sato. Opt. Commun., 5, 134 (1972).
19. P.P. Sorokin, J.R. Lankard and V.L. Moruzzi. Appl. Phys. Letters, 15, 179 (1969).
20. R. Flach, I.S. Shahin and W. . Yen. Appl. Opt., 13, 2095 (1974).
21. H. Kogelnik and C.V. Shank. Appl. Phys. Letters, 16, 152 (1971).
22. C.V. S hank, J.E. Bjorkholm and H. Kogelnik. Appl. Phys. Letters, 13, 395 (1971).

23. G. Dujardin and Y.H. Meyer *Opt. Commun.*, 24, 24 (1978)
24. I. Itzkan and F.W. Cunningham *I.E.E. J. QE-8*, 101 (1972).
25. J. Lawler, W. Fitzsimmons and L. Anderson. *Appl. Opt* 15, 1033 (1976).
26. T.G. Pavlopoulos. *Opt. Commun.*, 24, 170 (1978).
27. P.J. Sebastian and K. Sathianandan. *Proc. of Quant. Electron. Symposium, Poona.* (1981).
28. C.E. Moller, C.W. Verber and A.H. Adelman. *Appl. Phys. Letters*, 18, 273 (1971).
29. B.B. McFarland. *Appl. Phys. Letters* 10, 208 (1967).
30. C.H. Dugan, A. Lee and F.J. Morgan. *Appl. Opt.* 17, 1012 (1978).
31. F.J. Morgan and M. Dugan. *Appl. Opt.* 18, 4112 (1979)
32. F.P. Schafer. *Dye Lasers*, eds. F.P. Schafer (Springer Verlag, 1977) p. 47.
33. F.P. Schafer, *Dye Lasers*, eds. F.P. Schafer (Springer Verlag, 1977) p. 49.

CHAPTER IV

ENERGY TRANSFER STUDIES IN DYE LASERS

ABSTRACT

The lasing characteristics of the mixed dye systems of Rhodamin 6G - Safranin T, Rhodamin 6G - Rhodamin B and Coumarin 120 - Rhodamin 6G were studied using N<sub>2</sub> laser as the pumping source. Laser action was obtained from Safranin T in the mixed dye system with a concentration tuning range of 31 nm. The lasing peak wavelengths as a function of the concentration of the donor and the acceptor were studied for all the three systems. The observed donor concentration dependence on the emission peak wavelengths was attributed to the formation of a complex in the dye mixtures. The blue shift of the emission peaks as a result of donor sensitization was investigated. This blue shift also was found dependent on donor concentration. An enhancement of the power output of the order of 200% in Rh-6G - Rh-B mixture and 50% in C 120 - Rh-6G mixture was observed. A 1:1 molar concentration of donor and acceptor was found to give the maximum efficiency. The degree of polarization of the EFDL output was measured as a function of the concentration of the donor and the acceptor. The amount of depolarization introduced by energy transfer mechanism was experimentally obtained.

#### 4.10 Introduction

The increasing applications of dye lasers in spectroscopy and photochemistry demand the improvement of efficiency and extension of spectral region of operation of the dye lasers. Much work has been reported recently in this direction by the excitation of dyes by energy transfer processes. Nitrogen laser pumped dye lasers are limited to dyes which absorb the  $N_2$  laser or to pumping schemes where the excitation energy is transferred from an absorbing donor to an acceptor. Therefore, Energy transfer dye laser (ETDL) and laser induced intermolecular and intramolecular processes have become the subject of intense study.<sup>4-35</sup> In the present chapter a short review of the work done on ETDL and the characteristics of some specific donor - acceptor pairs are reported.

#### 4.20 A Review of the Work on ETDL

Several reports<sup>1-3</sup> concerning the theoretical and experimental aspects of excitation transfer have appeared during the last decade, but only recently extensive discussions of its applications in ETDL systems have been reported.<sup>4-31</sup> In 1968, soon after the discovery of organic dye solution lasers, Peterson et al.<sup>4</sup> demonstrated the feasibility of a dye mixture laser with flash lamp excitation. In 1971 Joeller et al.<sup>1</sup>

obtained effective excitation transfer from Rh-6G to Cresyl violet by  $N_2$  laser pumping and observed an increase in power output. A simple theoretical model developed by Dienes et al.<sup>6</sup> is found to be in good agreement with the experimental results obtained for Cresyl violet--Rh-G mixture, a common pair used for most of the ETDL studies.<sup>4-7</sup> They could also explain the gain variation with acceptor concentration with this theoretical model. The gain measurements done by them on Rh-6G - Cresyl violet mixture and Cresyl violet alone clearly show a high gain in the mixture as compared to Cresyl violet alone. This high gain of ETDL system was demonstrated in other donor-acceptor pairs also such as Rh-6G -- Rh-B<sup>3</sup>, Coumarin 30 -- Rh-6 and Bis - MSB--Perylene.<sup>10</sup> As a result of this high gain, the conversion efficiency of dye laser will be improved much. Recently, the author obtained a conversion efficiency of 21% for the dye mixture Rh-6G - Rh-B<sup>3</sup> at a bandwidth of 1 Å whereas the same for Rh-B alone was only 7%. It is interesting to note that dyes like perylene could be lased by energy transfer mechanism which otherwise would not have been possible. This high gain, which is the result of an enhanced life time of the sensitized acceptor,<sup>9</sup> produces a blue shift in the emission peak of the dye. Recent investigations on  $N_2$  laser pumped ETDL showed pronounced blue shift in the superradiant peak emission wavelengths of Rh-6G, Rh-B, Brilliant sulphafavin, Coumarin - 1 and Perylene.<sup>9,11,12</sup> If the fluorescent

levels of donor and acceptor are closely located, this blue shift makes it difficult to identify the lasing species. In such systems, as suggested by Kusumoto et al.,<sup>13</sup> the lasing species is identified as the one whose emission peak is independent of the other. But the author showed that this rule cannot be applied, since in many mixture systems the emission peak is dependent on donor concentration.<sup>12</sup>

Many authors have tried to determine the prominent mechanisms of energy transfer in ETDL systems.<sup>7,9,10,13-15</sup> The prominent mechanisms of energy transfer are the radiative transfer, resonance transfer due to long range dipole - dipole interaction and the collisional transfer. Lin and Dienes<sup>7</sup>, by measuring the acceptor concentration and solvent dependence of the fluorescence life time of the donor in Rh-6G - Cresyl violet mixtures, determined the reaction rate constant of resonance transfer and concluded that this mechanism was dominant compared to the collisional transfer. Milburn and Brayman<sup>15</sup> reported a significant contribution of radiative transfer by measuring the spatial distribution and the time dependence of simultaneous two wavelength output in Rh-6G - Cresyl violet mixture. A quantitative study corresponding to radiative transfer and resonance transfer is reported by Urisu and Kajiyama.<sup>9</sup> From the concentration dependence of the effective fluorescence life time they determined the rate constants for both the processes and have shown that radiative

transfer is prominent in Coumarine 30 - Rh-6G mixture. The dominance of these energy transfer mechanisms in a given dye mixture may depend on the concentration and the solvent.<sup>10,14</sup>

One of the main advantages of ETDL systems over conventional dye lasers is the extension of the spectral region of operation. An efficient energy transfer process occurs in a dye mixture when the wavelength region of emission of the donor overlaps the absorption of the acceptor. In order to get laser action from a dye by N<sub>2</sub> laser pumping, either the donor or the acceptor need be a lasing dye under N<sub>2</sub> laser pumping as in the case of Rh-6G - Safranin T,<sup>17</sup> anthracene - Perylene<sup>10</sup> and Coumarin - Acriflavin.<sup>16</sup> Pavlopoulos<sup>18</sup> has discussed the requirement for an efficient donor dye for flash lamp pumped ETDL. Dunning and Stokes<sup>19</sup> have reported near infrared laser emission from DODC with Rh-B as the donor under N<sub>2</sub> laser pumping. The author could get an enhanced tuning range for Rh-6G by energy transfer mechanism because of the low threshold lasing in ETDL.

In an energy transfer process, it is usual that the donor fluorescence will be quenched by the acceptor. But by a proper selection of the dyes and their concentration it is possible to get simultaneous laser action from both the donor and the acceptor. Ahmed et al.<sup>16</sup> demonstrated the feasibility of a white light dye laser by energy transfer mechani-

He obtained simultaneous lasing at three primary colours from 7-diethylamino-4-methylcoumarine, Acriflavin and Rh-B, thus showing that a cascade process of energy transfer is efficient. Many of the spectroscopic applications require simultaneous multiple wavelength laser lines from a laser system. A suitable design of the resonator will permit such an operation of a dye laser, but the wavelength will be within the range of a single dye. For widely separated multiple wavelength operation of a dye laser energy transfer mechanism using mixed dyes is the only possible solution reported so far.

The various advantages of energy transfer mechanism in dye lasers attracted the attention of many researchers. However, a proper theoretical approach to the problem is yet to be worked out in detail. An attempt was made by Dienes and Madden<sup>6</sup> to give a simple theoretical model for the performance of an ETDL. But a more accurate treatment on the performance of an ETDL was given by Weiss and Speiser<sup>20</sup> and a computer simulation applied to the Anthracene - Perylene system by Speiser and Katraro<sup>21</sup> shows good agreement with experimental results.

#### 4.30 Studies on some specific systems and their Performance

A detailed investigation on the performance characteristics of Rh-6G - Safranin I, Rh-6G - Rh-B and C 120 .

Rh-6G dye mixture systems are presented here. Since the acceptors in all the three mixtures are found to be lasing under energy transfer conditions, all the experimental observations are based on the lasing mode of the dyes.

#### 4.31 Rh-6G - Safranin T

The molecular structures of Rh-6G ( $C_{23}H_{31}ClN_2O_3$  molecular weight 479.02) and Safranin T ( $C_{20}H_{19}N_4Cl$ -molecular weight 326.1) are shown in Fig. 4.1 and 4.2 respectively. Both the dyes belong to the Xanthere group of dyes. Laser action from Safranin T, was reported previously<sup>34</sup> using 530 nm second harmonic radiation of Nd - glass laser as the pump source. But for the present investigations initial attempts made to lase Safranin T using  $N_2$  laser were unsuccessful. The most important criteria for an efficient energy transfer in a dye mixture is the overlap of the emission spectrum of the donor and absorption spectrum of the acceptor. The studies on spectral characteristics of Rh-6G emission and Safranin T, absorption showed a good spectral overlap and laser action was obtained from Safranin T, by energy transfer process with Rh-6G as the donor using  $N_2$  laser as the pump source.

Rh-6G (LOBA - India) and Safranin T (Riedel - Germany) were used without further purification. Spectro

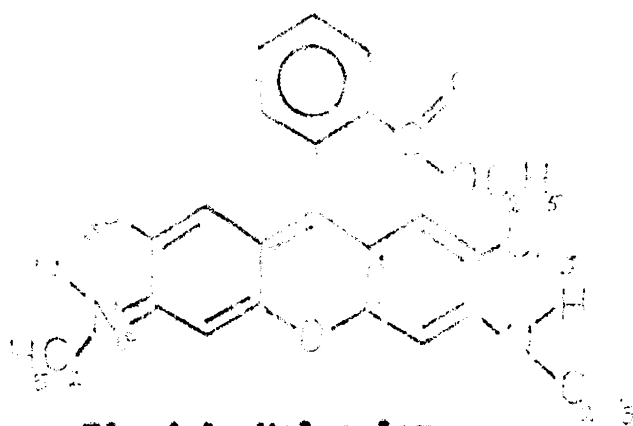


**Fig.4.1. Molecular structure of Rh 6G.**

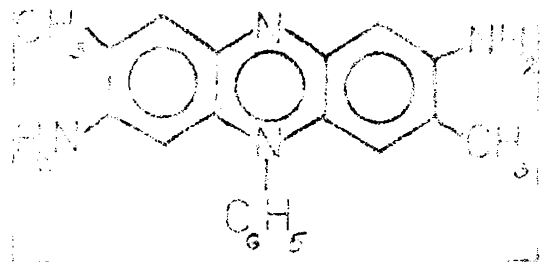


**Fig. 4.2. Molecular structure of Safranin T.**

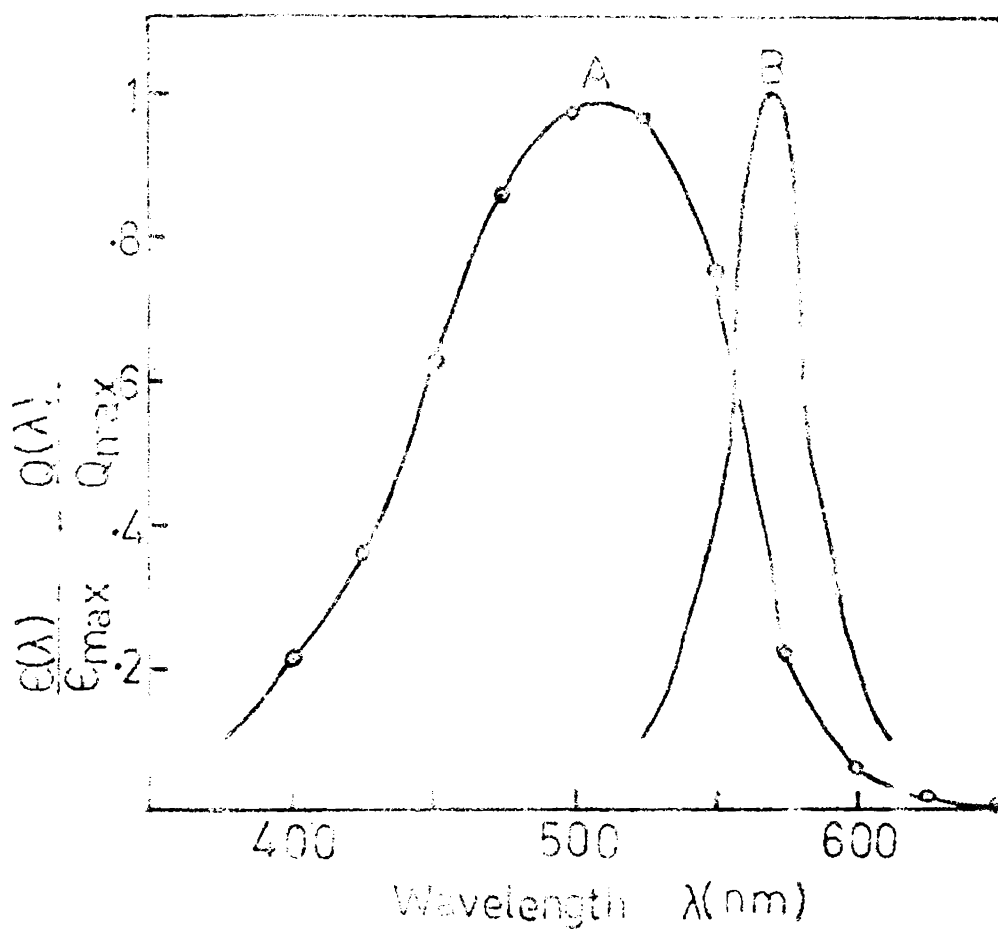


**Fig.4.3. Absorption spectrum of Safranin T (A) and Emission spectrum of Rh 6G (B).**

grade Methanol was used as the common solvent. The absorption spectrum of Safranin T was obtained with a systronics spectro calorimeter for an absorption path length of 1 cm and concentration of 0.013 gram/litre and is shown in Fig. 4.3(A). The absorption peak was found to be at 515 nm and the spectrum extended up to 625 nm.

The dye solution was transversely pumped and laser in a superradiant manner by 337.1 nm radiation from a pulsed  $N_2$  laser (CEL - HL 103) with an output peak power of 100 kW at a repetition rate of 30 pps. The fluorescence spectra of 0.6 gram/litre Rh-6G in methanol and the superradiant emission peaks ( $\lambda_{max}$ ) of Rh-6G alone and Rh-6G - Safranin T mixture were measured by a prism monochromator, an EMI 9694 QB photomultiplier and a nanometer. The fluorescence emission spectrum of Rh-6G is shown in Fig. 4.3 (B) which shows a good spectral overlap with the absorption spectrum of Safranin T.

The concentration effect of Rh-6G on the  $\lambda_{max}$  is shown in Fig. 4.4 (A). Fig. 4.4 (B) represents the change in  $\lambda_{max}$  of Safranin T with concentration for a fixed Rh-6G concentration of 1.2 grams/litre while Fig. 4.4 (C) gives  $\lambda_{max}$  for different concentrations of Rh-6G with a fixed concentration of Safranin T (1 gram/litre).

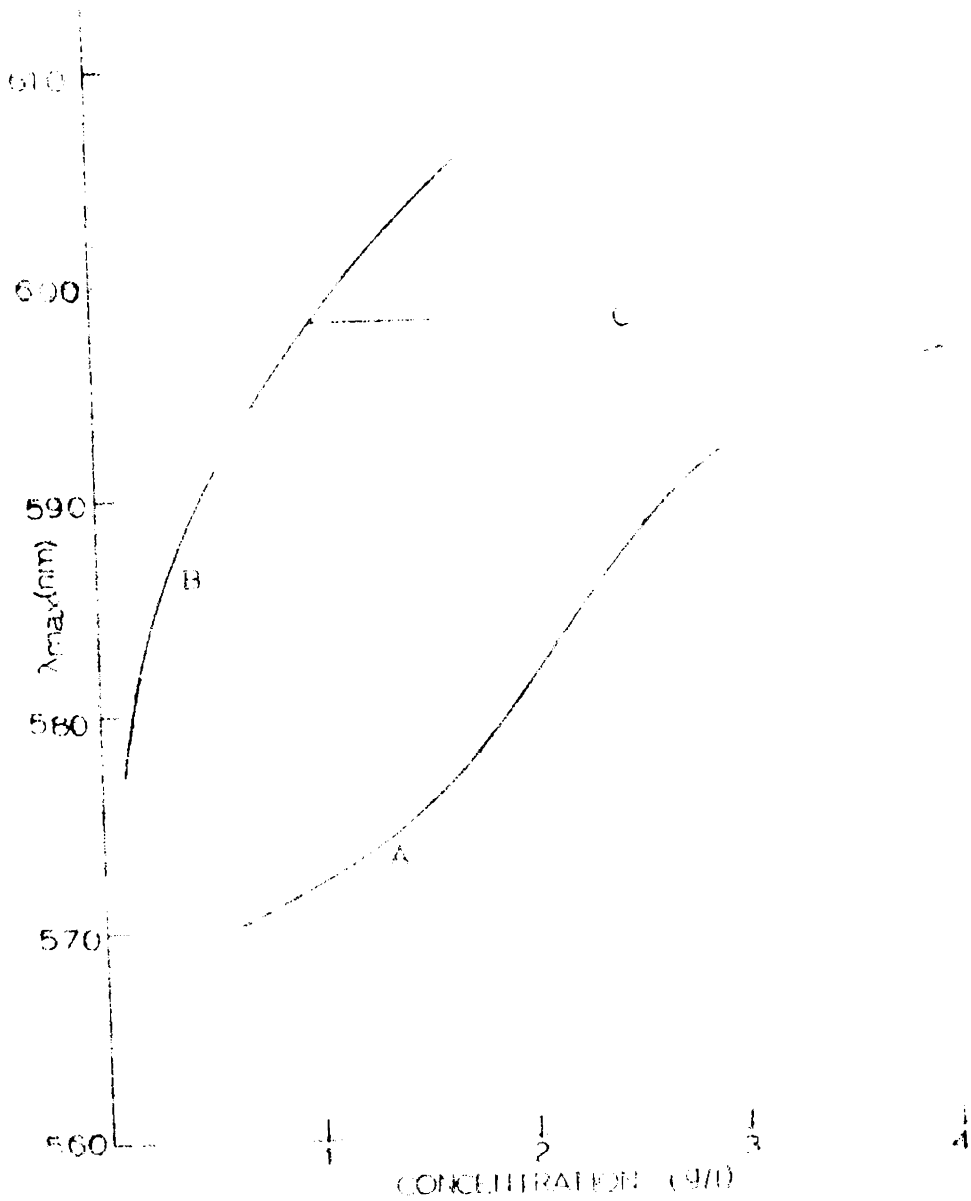


**Fig.4.4. Plots of lasing  $\lambda_{\max}$  versus concentration.**  
**(A) Rh 6G alone. (B) Safranin T with a fixed concentration of 1.2 grams/litre. (C) Rh 6G with a fixed Safranin T concentration of 1 gram/litre.**

Fig. 4.4 (C) clearly demonstrates that the  $\lambda_{\max}$  depends only on the concentration of Safranin T establishing the fact that the lasing takes place in Safranin T. Thus most of the excitation energy absorbed by Rh-6G is transferred to Safranin T as a useful pump power making excitation transfer quite efficient. Moreover the fact that an  $N_2$  laser of 100 kW is used to lase Safranin T by energy transfer with the concentration tuning range of 31 nm further demonstrates that the ETDL system can work efficiently, even at very low pump powers.

The  $\lambda_{\max}$  value of Safranin T in the ETDL system at the concentration of 2 gram/litre is at 608 nm. Further increase in the concentration of Safranin T stopped the lasing action even at higher donor concentrations. Safranin T alone is reported to lase at 610 nm.<sup>34</sup> But in the present investigations the 610 nm peak emission could not be obtained. The reason for this may be the blue shift of a donor sensitized laser system compared to an unsensitized system. Such an effect was observed by Klenerman et al.<sup>11</sup> and theoretically explained by Urisu et al.<sup>9</sup> But a quantitative estimate of this blue shift could not be obtained since Safranin T alone was not lasing under  $N_2$  laser pumping.

4.32 Rh-6G - Rh-B

Unlike the Rh-6G - Safranin T system the dye pair Rh-6G - Rh-B is a well known system for its efficiency of transferring energy from Rh-6G to Rh-B and both the dyes can be lased individually by  $N_2$  laser pumping. Hence the system was used to study the performance of a typical ETDL. The molecular structure of Rh-B (molecular weight 470) is shown in Fig. 4.5.

The donor and acceptor concentration dependence on the superradiant emission peaks of the ETDL system was obtained with the setup described in 4.31. with a modification that the prism monochromator was replaced by a Jarrell - Ash 0.5 M scanning monochromator and the nanoameter by a Fisher-Recordall 5000 chart recorder. Fig. 4.6 (A) shows the concentration variation of  $\lambda_{max}$  values for Rh-B alone while Fig. 4.6 (B,C and D) represents the shifts in the Rh-B emission peak for different Rh-6G concentrations (0.2 g/l to 8 g/l) with three fixed Rh-B concentrations (3 g/l, 2 g/l and 1 g/l).

Two important results are evident from these observations. One is the blue shift of the emission peaks of donor sensitized Rh-B and the other is the donor concentration dependence of the emission peaks. A donor sensitized system is shown to have a higher gain compared to unsensitized system

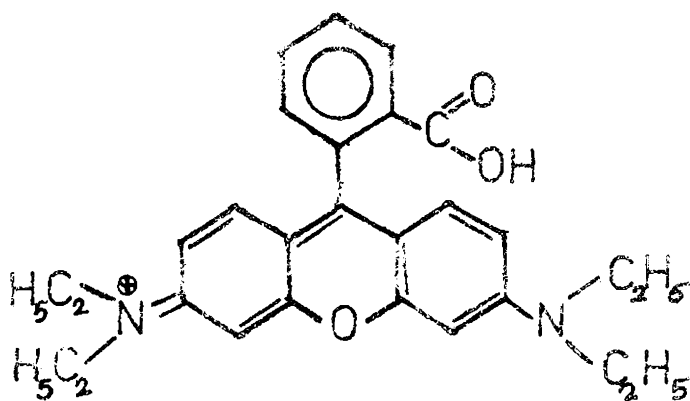


**Fig.4.5. Molecular structure of Rh B.**

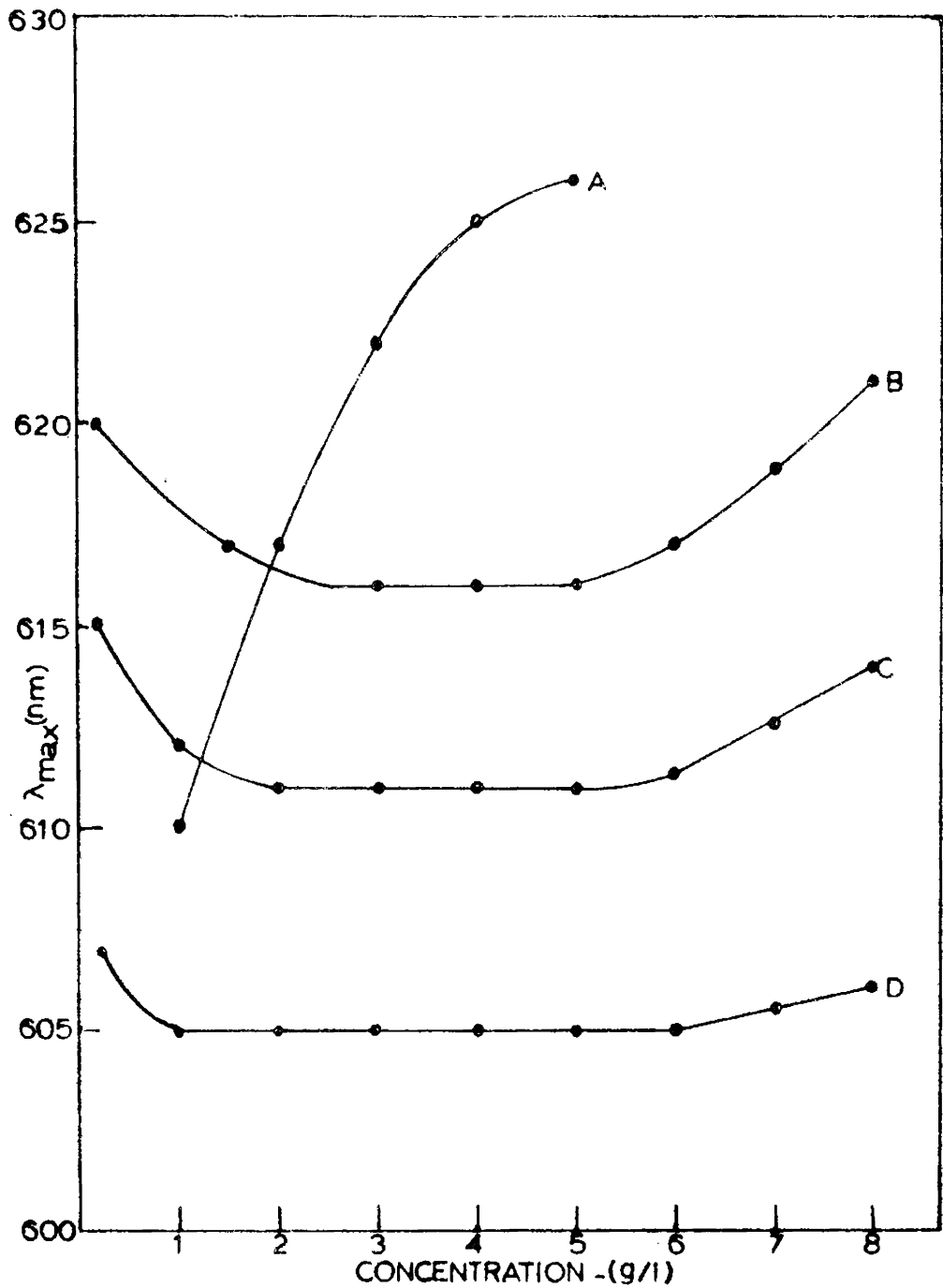


**Fig.4.6. Plots of lasing  $\lambda_{max}$  versus concentration. (A) Rh B alone. (B) Rh 6G-Rh B mixture with a fixed concentration of 3 g/l. (C) Rh 6G-Rh B mixture with a fixed Rh B concentration of 2 g/l. (D) Rh 6G-Rh B mixture with a fixed Rh B concentration of 1 g/l.**

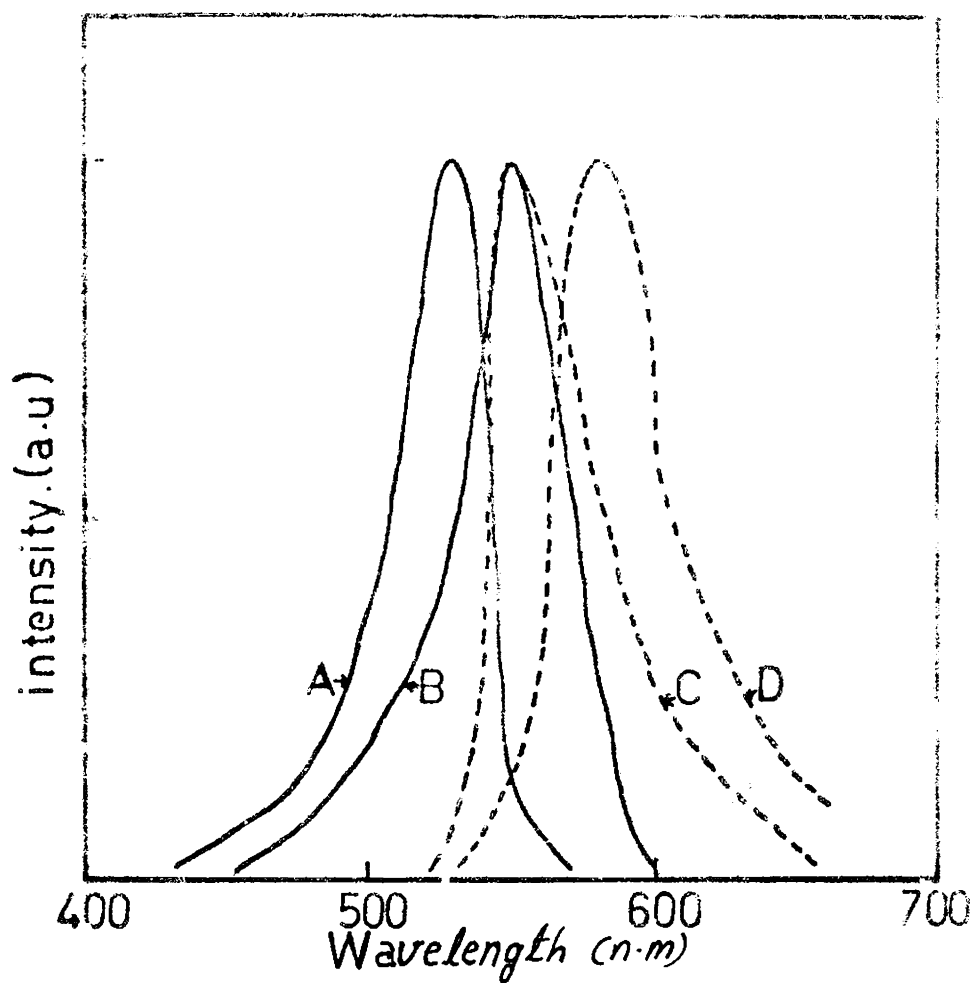


**Fig.4.7. Absorption and Emission spectra of Rh 6G and Rh B. (A) Absorption spectrum of Rh 6G. (B) Absorption spectrum of Rh B. (C) Emission spectrum of Rh 6G. (D) Emission spectrum of Rh B.**

system because of an increase in the effective life time of the acceptor.<sup>9</sup> As a result, the gain maximum will be shifted to blue region.<sup>35</sup> The life time of the acceptor will be appreciably increased at very low concentrations ( $<10^{-3}$  l/l) as reported by Urisu et al.<sup>9</sup> But this enhanced life time will remain approximately a constant at higher concentration of the acceptor as is evident in the case of Rh-6G - Rh-B where the maximum blue shift remains a constant ( $\sim 5$  nm) in the concentration range  $2 \times 10^{-3}$  l/l to  $6 \times 10^{-3}$  l/l (1 g/l to 3 g/l). Similar blue shifts have been reported in other dye mixture systems also.<sup>11</sup>

Fig. 4.6 (B,C and D) shows that this blue shift can be affected by the donor concentration. At very low concentrations of the donor only partial energy transfer is taking place. Since the intermolecular distance is very high the donor-acceptor interaction is very weak. Hence the long wavelength tail of Rh-6G emission where Rh-B has no absorption, as can be seen from Fig. 4.7 (the absorption and emission spectra of Rh-6G and Rh-B), is super imposed on the Rh-B emission and a blue shift is observed. In addition to this spectral overlap the enhancement of life time due to partial energy transfer also may contribute to this blue shift. But this blue shift is less compared to that caused by the enhanced life time due to complete energy transfer. It can be seen

that when the donor-acceptor concentration approaches 1:1 ratio the energy transfer becomes maximum and the blue shift due to enhanced life time also becomes maximum.

Another important observation is the red shift from the maximum blue shifted wavelength ( $\Delta\lambda$ ) at higher Rh-6G concentrations. This red shift may be attributed to a complex formation as it is evident from the nature of the red shift for different Rh-B concentration. Such a red shift due to complex formation, as in the case of a methanol solution of pyrylium and dimethyl aniline is not uncommon.<sup>36</sup> The experimental evidences are not in favour of a ground state interaction of organic dye molecules when organic solvents are used.<sup>37</sup> Hence these complexes are the result of excited state interactions (exciplex). A detailed investigation of the absorption and fluorescence properties of these exciplexes is necessary to explain its role in the observed red shift. The nature of  $\Delta\lambda$  variation at higher Rh-B concentrations than 3 g/l could not be obtained since under the present experimental conditions the system was not lasing. The rate of complex formation is limited by the diffusion of the two constituents and is proportional to the product of the concentrations of the constituents. The slopes of the red shift portion of B C and D are different. This indicates that the phenomenon depends on the concentration of donor as well as

the acceptor. The decrease in the maximum blue shifted region with increasing Rh-B concentration further supports the complex formation. This study shows that in the Rh-6G - Rh-B ETDL system the lasing  $\lambda_{\max}$  of Rh-B is dependent on Rh-6G concentration due to the formation of a complex. A similar donor concentration dependence of  $\lambda_{\max}$  of the acceptor was seen in the system C 120 - Rh-6G.

The tuning range that can be obtained with concentration variation of the lasing species was studied. Fig. 4.8 (A) shows the concentration variation of  $\lambda_{\max}$  values for Rh-B alone while Fig. 4.8 (B) represents the same for donor sensitized Rh-B. It can be seen that the tuning range for the ETDL system is approximately the same as that for non-sensitized system except for the blue shift. In Fig. 4.8 (B) the  $\lambda_{\max}$  values were obtained by keeping  $\frac{[D]}{[A]} = 1$  since it was the concentration ratio at which maximum efficiency could be obtained. Moreover this ratio allows the operation of the system on the maximum blue shifted region shown in Fig. 4.6 (BCD). In order to get laser action at acceptor concentration above 3 g/l the  $N_2$  laser power had to be increased from 100 kW to 150 kW where as the Rh-B alone system was lasing up to 5 g/l with 100 kW  $N_2$  power. The reason for this decreased efficiency of the donor sensitized system at higher donor and acceptor concentrations is fluorescence quenching by the formation of complexes.

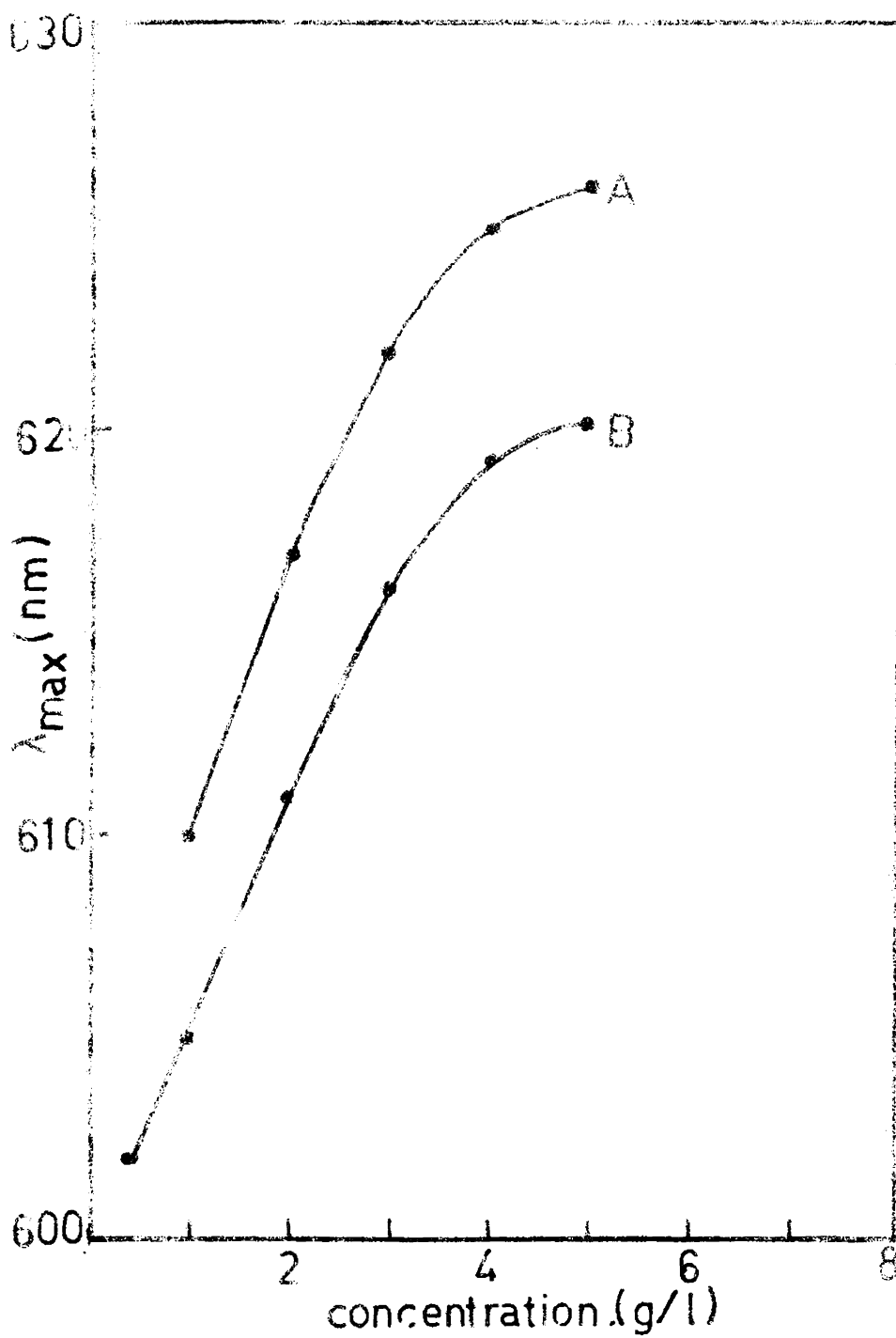


**Fig. 4.8. Tuning range of Rh B alone (A) and donor (Rh 6G) sensitized Rh B (B).**

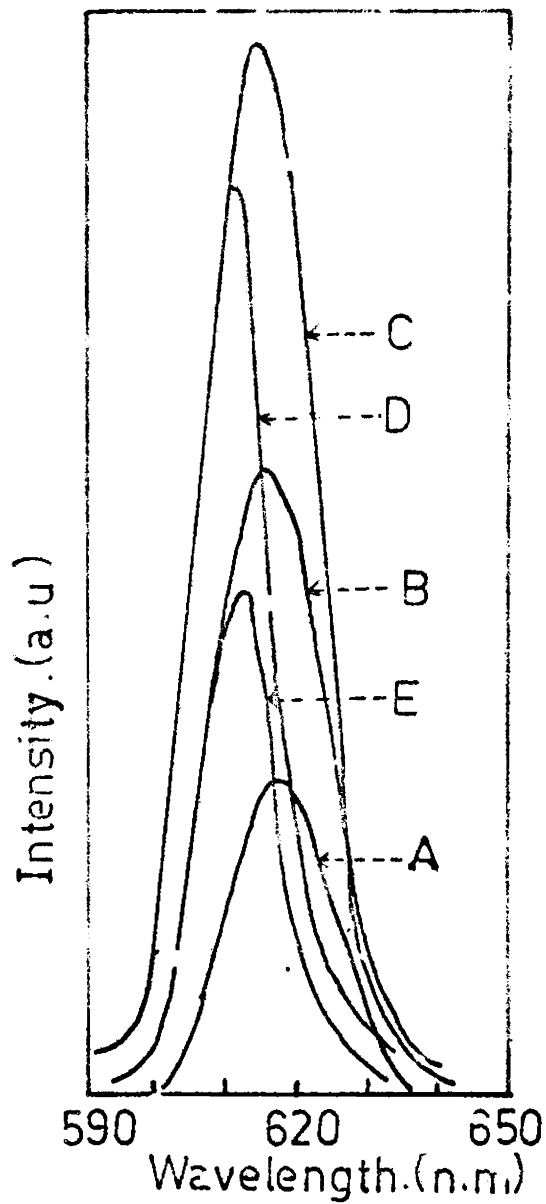


**Fig.4.9. Efficiency of Rh 6G - Rh B ETDL.**

- (A) Rh B alone 1.5 g/l.**
- (B) Rh B 1.5 g/l + Rh 6G 1 g/l.**
- (C) Rh B 1.5 g/l + Rh 6G 1.25 g/l.**
- (D) Rh B 1.5 g/l + Rh 6G 2 g/l.**
- (E) Rh B 1.5 g/l + Rh 6G 8 g/l.**

The efficiency of the ETDL system, in terms of intensity, as a function of donor concentration is shown in Fig. 4.9. It can be seen that as the donor concentration increases the intensity of the peak emission wavelength increases. When the donor acceptor concentration approaches 1:1 ratio the peak intensity becomes maximum. A further increase in the donor concentration decreases the peak intensity. This shows that the linear dependence of intensity on donor concentration, as predicted by Speiser et al.<sup>21</sup> is valid only at lower concentrations of the donor. At higher donor concentrations this linear dependence is disturbed and shows a decrease in intensity due to complex formation. A 200% increase in intensity for the sensitized system (Fig. 4.9(C)) compared to the unsensitized system (Fig. 4.9(A)) was observed. This shows that the ETDL is more efficient than the conventional dye laser.

The studies on the polarization properties of the ETDL, Rh-6G - Rh-B, has given the extent of depolarization introduced by energy transfer mechanism which is a well known depolarizing factor.<sup>37</sup> The degree of polarization of the Rh-B emission as a function of concentration was measured with the monochromator, PII, chart recorder and the perpendicular and parallel polarizing filters. The ETDL was operated in a superradiant manner and the degree of polarization  $P = \frac{I_{\parallel} - I_{\perp}}{I_{\parallel} + I_{\perp}}$

was measured at the emission peaks. The pumping  $N_2$  laser power was monitored by a photodiode and oscilloscope. No correction factor was applied to the calculated 'P' values for the degree of polarization introduced by the monochromator since it will be less than 1%. The partially polarized  $N_2$  laser used for the excitation of the dye was having a degree of polarization  $P = + 0.33$ . The solvent was methanol.

Fig. 4.10(A) shows the variation of the degree of polarization of Rh-B with concentration and Fig. 4.10 (B) shows that for the dye mixture Rh-6G - Rh-B for a fixed concentration of 2.4 g/l of Rh-6G. The drop in the degree of polarization at higher concentration of Rh-B is due to the concentration depolarization. The relative orientation between the absorbing and emitting dipole causes the depolarization. At higher concentration the absorbed quantum of light is transferred from one oscillator to another with a certain angle between them. This further enhances the depolarization. In the mixed dye system it can be seen that the polarization changes in a complicated manner with increasing acceptor concentration for a fixed donor concentration. Energy transfer takes place preferentially between parallel dipoles, but non parallel dipoles also undergo transfer with resulting depolarization. This effect can be observed from Fig. 4.10 (A,B) which shows a drop in the degree of polarization of the donor

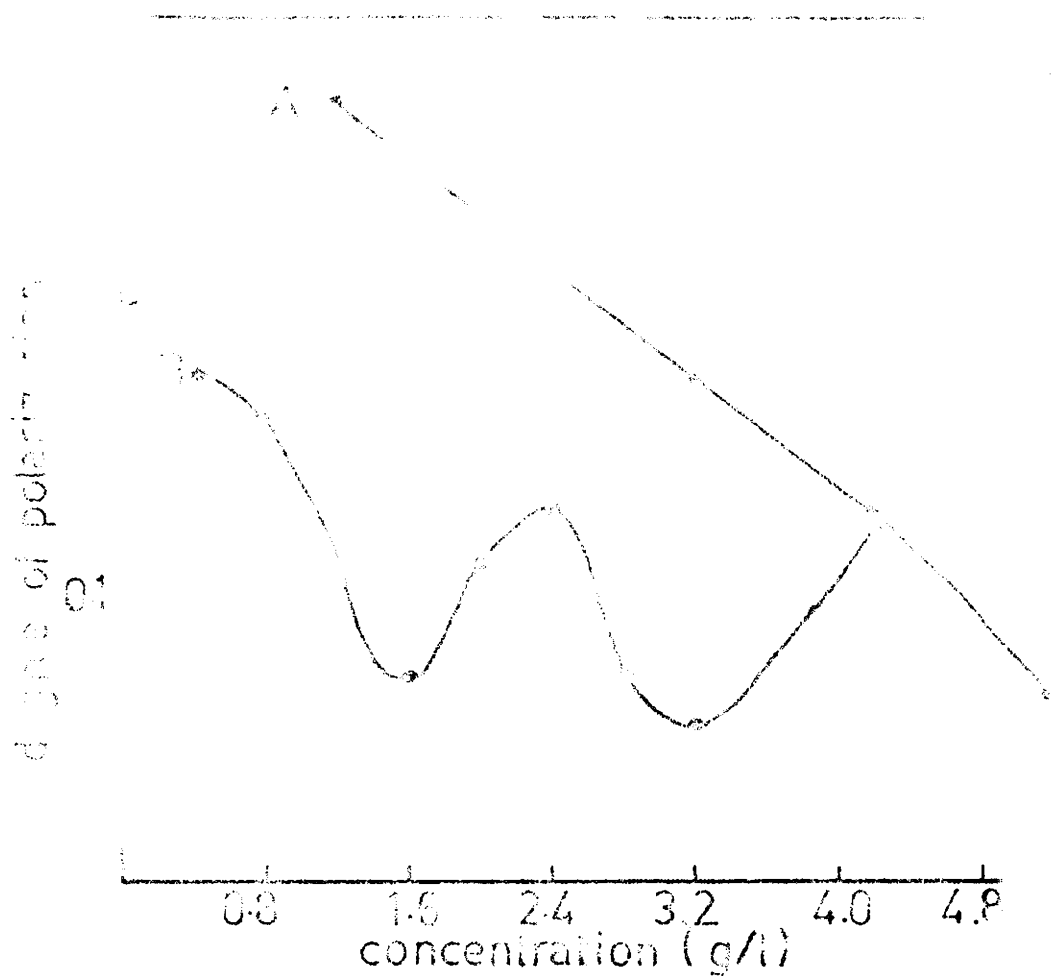


**Fig.4.10.** The degree of polarization as a function of concentration. (A) Rh B alone. (B) Rh 6G-Rh B mixture for a fixed Rh 6G concentration of 2.4 g/l.

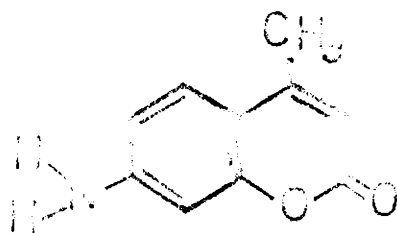


**Fig.4.11.** Molecular structure of Coumaxin 120.

sensitized system compared to the unsensitized system. However at very high acceptor concentration compared to that of the donor this drop in polarization is zero. To give a satisfactory explanation for this and the complicated variation of polarization with acceptor concentration, further investigations are needed.

#### 4.33 C 120 - Rh-6G

The system C 120 - Rh-6G is a best example for efficient energy transfer between a Coumarin derivative and a Xanthene dye. The molecular structure of C 120 (Molecular wt.175) is shown in Fig. 4.11. The ETDL performance of the system was found in good agreement with that of Rh-6G - Rh-B.

Fig. 4.12 (B) shows the concentration dependence of  $\lambda_{\max}$  of Rh-6G for a fixed C 120 concentration of 0.35 g/l in methanol and Fig. 4.12 (A) that of Rh-6G alone. At lower concentrations of Rh-6G the blue shift introduced due to donor sensitization is small whereas the same at higher concentration is comparatively large. This indicates that the change in life time of donor sensitized Rh-6G from nonsensitized Rh-6G at higher concentration is large compared to the change at lower concentration since the blue shift is due to the enhancement of acceptor life time.<sup>9</sup> It is a well know fact

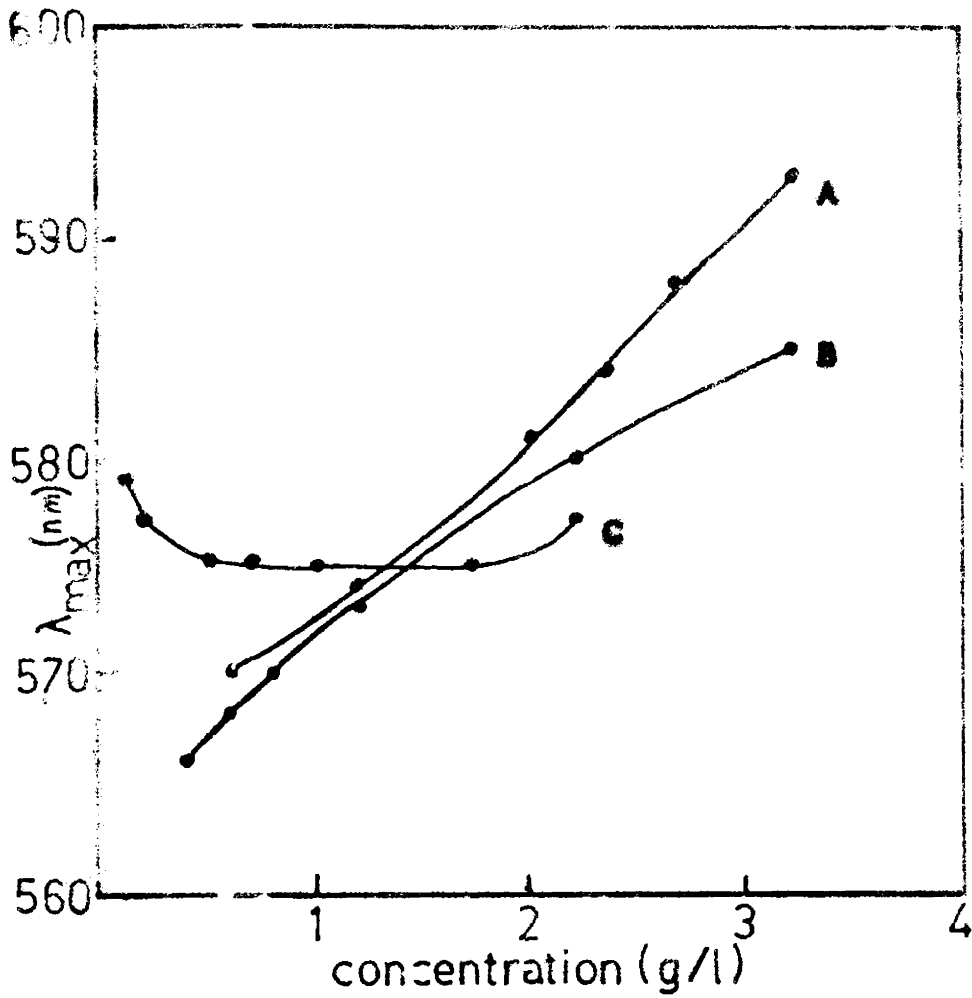


**Fig.4.12. Plots of lasing  $\lambda_{max}$  versus concentration .**  
**(A) Rh 6G alone. (B) C 120 - Rh 6G mixture**  
**with a fixed C 120 concentration of 0.35 g/l.**  
**(C) C120 - Rh 6G mixture with a fixed Rh 6G**  
**concentration of 2 g/l.**

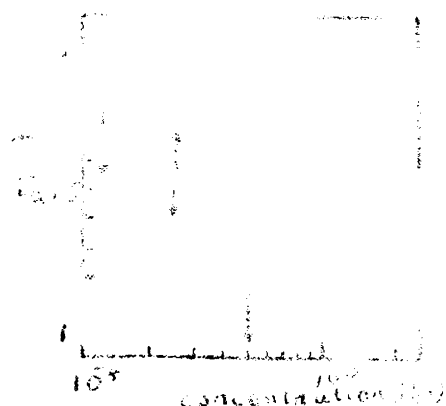


**Fig.4.14.** The concentration dependence of the effective fluorescence life time  $\tau_{ef}$  of donor (C 30) sensitized Rh 6G in methanol.  $\tau_{ef}$  is normalized by the fluorescence life time  $\tau_0$  of pure Rh 6G.

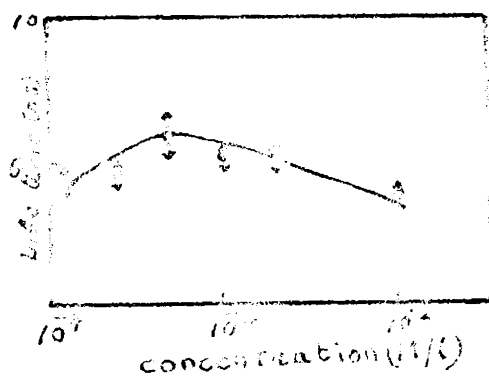


**Fig.4.13** Concentration dependence of the fluorescence life time of Rh 6G.

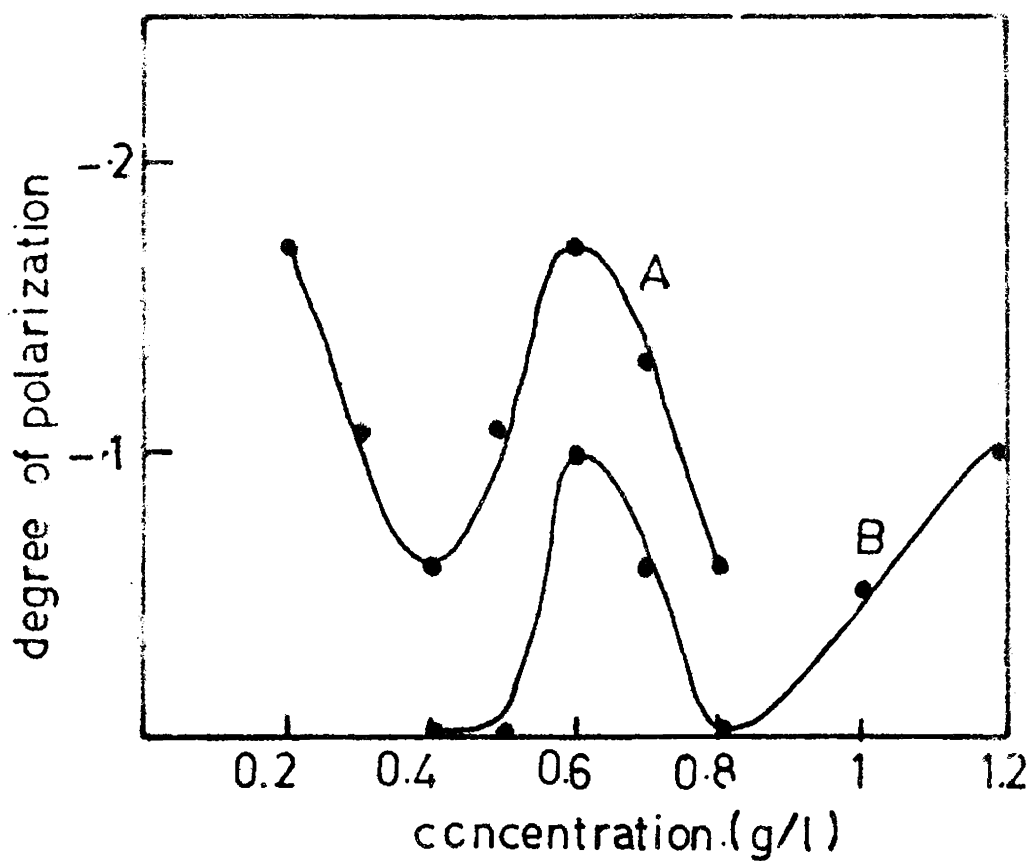
that Rh-6G in Methanol shows an increase in life time with increasing concentration upto  $5 \times 10^{-4}$  M/l due to radiation trapping and then a decrease with further increase in concentration due to concentration quenching. The nature of this dependence is shown in Fig. 4.13.<sup>35</sup> The concentration dependence of the life time of the donor (C 30) sensitized Rh-6G in methanol is shown in Fig. 4.14<sup>9</sup> where  $\tau_{ef}$  is the life time of donor sensitized Rh-6G and  $\tau_a$  is that of pure Rh-6G. It is evident from Fig. 4.13 and 4.14 that donor sensitized Rh-6G shows the maximum change in life time at concentrations in which life time of pure Rh-6G is the least. Since the blue shift of  $\lambda_{max}$  in ETDL is due to the enhancement of life time of acceptor the maximum blue shift will be observed when the change in life time is a maximum. In the lower concentration range ( $10^{-4}$  to  $2 \times 10^{-3}$  M/l) of C 30 + Rh-6G this effect was confirmed by Urisu et al.<sup>9</sup> But from the increasing blue shift in the range  $1.25 \times 10^{-3}$  to  $6.25 \times 10^{-3}$  M/l observed, in the present investigations, it is evident that the life time of donor sensitized Rh-6G enhances with respect to that of pure Rh-6G in the concentration range.

Fig. 4.12 (C) shows the donor concentration dependence of Rh-6G peak emission wavelength. Rh-6G concentration is fixed at 2 grams/litre ( $4 \times 10^{-3}$  M/l) and this concentration of pure Rh-6G has the  $\lambda_{max}$  at 581 nm. The blue shift due to

donor sensitization reaches a maximum only at a ratio of 1:1 molar concentration of C 120 and Rh-6G, (ie. at C 120 concentration 0.7 grams/litre =  $4 \times 10^{-3}$  M/l) as in the case of Rh-6G Rh-2. The gradual increase of this blue shift is only due to the enhancement of life time as a result of partial energy transfer since there was no overlap between the emission spectra of Rh-6G and C 120. The maximum blue shift remains a constant in the range  $4 \times 10^{-3}$  to  $10^{-2}$  M/l. The red shift with further increase in donor concentration suggests the possibility of formation of complexes in the dye mixture.

The measured output intensity of the ETDL was found to be a maximum when the molar concentration of C 120 and Rh-6G were approximately equal and was about 50% larger than that of pure Rh-6G.

The donor and acceptor concentration dependence of the degree of polarization of the system was studied and is shown in Fig. 4.15 (A) and 4.15 (B) respectively. The degree of polarization of the  $N_2$  laser was + 0.33, C 120 alone was + 0.26 at a concentration of  $2 \times 10^{-3}$  M/l and that of Rh-6G alone at a concentration of  $5 \times 10^{-3}$  M/l was - 0.27. C 120 and Rh-6G alone systems did not show any appreciable change in the degree of polarization in the concentration range investigated. Eventhough the nature of donor and acceptor concentration dependence cannot be explained, it is quite interesti



**Fig.4.15.** The degree of polarization as a function of concentration. (A) C 120-Rh 63 mixture with a fixed Rh 63 concentration of 1 g/l. (B) C 120-Rh 63 mixture with a fixed C 120 concentration of 0.35 g/l.

to see that the difference in the degree of polarization between donor and acceptor concentration dependence has an approximately constant value throughout the concentration range studied.

#### 4.34 Discussion

Since the first report on  $N_2$  laser pumped ETDL by Moeller et al. the art of ETDL has developed very rapidly. But even now the performance of ETDL is not fully known owing to the complexity of the quantum mechanical problem associated. Many authors have tried to give more or less simple models that are capable of explaining many experimental observations. The present investigations aimed at revealing many of the unattended or partially attended fields of ETDL was fruitful to a certain extent. The results of the investigations on the three specific ETDL systems can be summarized as follows.

The studies on Rh-6G - Safranin T shows that even if the acceptor dye has little or no absorption in the  $N_2$  laser wavelength it can be lased by energy transfer mechanism with a suitable donor. The selection of donor should be such that its emission spectrum must overlap the absorption spectrum of the acceptor. Because of the low threshold lasing in ETDL even if the acceptor dye has a fluorescence quantum efficiency substantially below unity laser action can be obtained from

the dye. On the other hand if the acceptor can be lased by direct excitation with  $N_2$  laser it can be lased with a lower pump power in ETDL as observed in the case of Rh-6G - Rh-B.

Eventhough Rh-6G, Safranin T and Rh-B are all from the Xanthene group of dyes, C 120 is from a different family. The C 120 - Rh-6G ETDL shows that efficient energy transfer is possible between a Coumarin derivative and a Xanth dye for laser action.

It can be seen that in all the three systems donor sensitization causes a blue shift in the emission peaks of the acceptor due to an enhancement of life time of the acceptor. Hence it has to be believed that the energy transfer mechanism effectively competes with the life time reducing mechanisms like concentration quenching. From the present investigations and the observations of Urisu et al.<sup>9</sup> it is clear that when the change in the effective life time of the acceptor is a maximum the blue shift is also a maximum. Hence the extent of blue shift can be taken as a measure of the change in life time.

If the fluorescent levels of donor and acceptor are closely located, the blue shift makes it difficult to identify the lasing species. In such systems, usually the

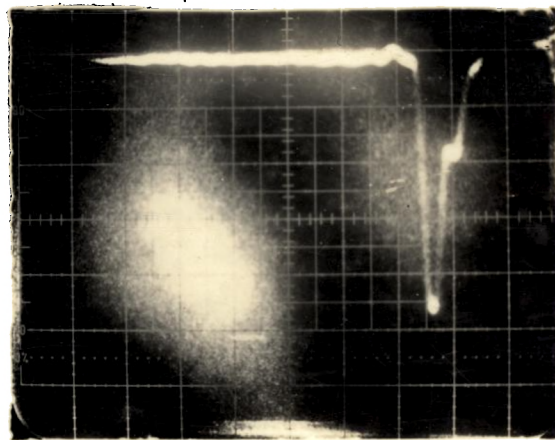
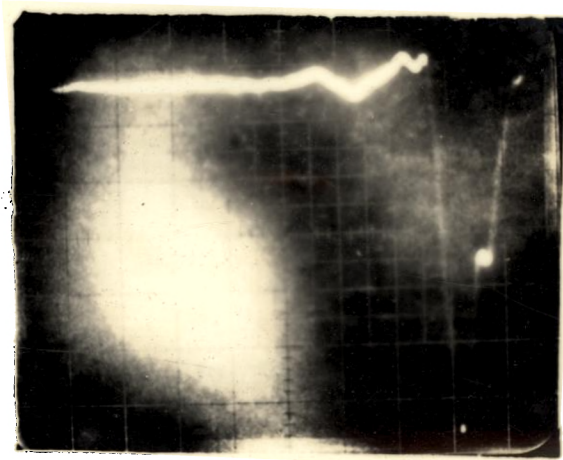
lasing species is identified as the one whose emission peak is independent of the concentration of the other. But the present investigations shows that the lasing peak wavelength of the acceptor can be dependent on the donor concentration also. Hence an investigation of the donor dependence on the acceptor emission becomes necessary prior to the identification of the lasing species. The donor concentration dependence on  $\lambda_{\max}$  have similar nature both in Rh-6G - Rh-B mixture and C 120 - Rh-6G system and this dependence is attributed to the formation of 'exciplex' in the systems eventhough its role on the donor dependence is not known.

The concentration tuning range of the ETDL systems is approximately the same as that of conventional dye lasers. However ETDL have the advantage that the acceptor can be lased even at very low concentrations, which otherwise would not have been possible, there by obtaining the shorter wavelength operation of the acceptor. This can be seen in the case of Rh-6G - Rh-B and C 120 - Rh-6G.

The most attractive feature of an ETDL is its power conversion efficiency. A 200% increase in the superradiant output power, in the case of Rh-6G - Rh-B system, and a 50% increase in the case of C 120 - Rh-6G was observed compared to the non-sensitized systems. In both the cases the maximum efficiency was obtained when the donor

acceptor molar concentration ratio was 1:1. This shows that even if a dye can be directly pumped by  $N_2$  laser it is better to use with a suitable donor for higher efficiency.

Eventhough the observed polarization properties of the ETDL systems can not be explained at this stage it gives us a measure of the depolarization introduced by energy transfer mechanism.



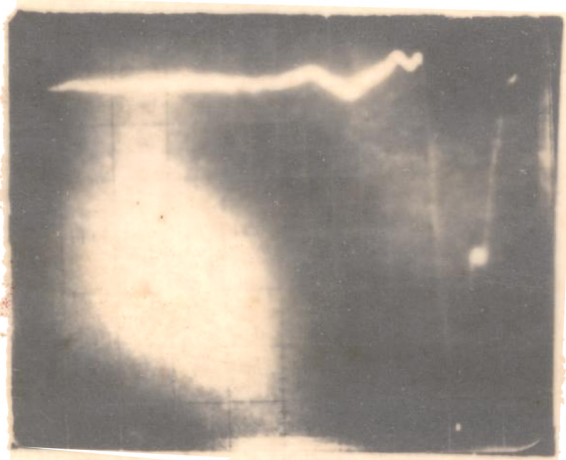


*Plate 1*

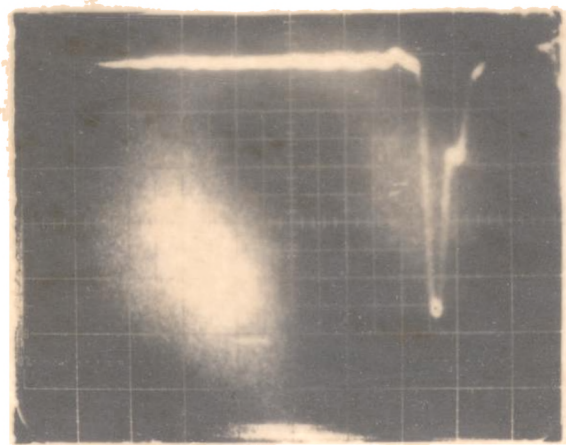


*Plate 2.*

References

1. D.L. Dexter, J. Chem. Phys. 21, 335 (1953).
2. Th. Forster, Discussions Faraday Soc., 27, 7, (1959).
3. P. Livingston, J. Phys. Chem. 61, 360 (1957).
4. O.G. Peterson and E.B. Snively, Bull. Am. Phys. Soc., 13, 397 (1968).
5. C.E. Moller, C.W. Verber and A.H. Adelman, Appl. Phys. Letters, 13, 278 (1971).
6. A. Dienes and M. Madden, J. Appl. Phys. 44, 4161 (1973).
7. C. Lin and A. Dienes, J. Appl. Phys. 44, 5050 (1973).
8. F.J. Sebastian and K. Sathianandan, Proc. of Quant. Electron, Symposium, Poona (1981).
9. T. Urisu and K. Kajiyama, J. Appl. Phys. 47, 3563 (1976).
10. I.B. Berlman, A. Rokni and C.R. Goldschmidt, Chem. Phys. Letters, 22, 458 (1973).
11. M. Kleinerman and H. Dabrowski, Opt. Commun. 26, 81 (1973).

12. P.J. Sebastian and K. Sathianandan, Opt. Commun. 35, 113 (1980).
13. Y. Kusunoto, H. Sato, K. Maeno and S. Yahiro, Chem. Phys. Letters 53, 383 (1978).
14. G.A. Kenney Wallace, J.H. Flint and L.C. Wallace Chem. Phys. Letters, 32, 71 (1975).
15. R.C. Hilborn and H.C. Brayman J. Appl. Phys. 45, 4912 (1974).
16. S.A. Ahmed, J.G. Gergely and D. Infante, J. Chem. Phys. 61, 1534 (1974).
17. P.J. Sebastian and K. Sathianandan, Opt. Commun. 32, 422 (1980).
18. T.G. Pavlopoulos Opt. Commun, 24, 170 (1973).
19. F.B. Dunning and E.D. Stokes. Opt. Commun. 6, 160 (1972).
20. E. Weiss and S. Speiser. Chem. Phys. Letters 40, 220 (1976).
21. S. Speiser and R. Katrarro, Opt. Commun. 27, 237 (1978).

22. E. Weiss and S. Speiser, Chem. Phys. Letters 42, 220 (1976).
23. K. Nagashima and T. Asakura, Opt. Commun. 19, 7 (1976).
24. P. Burlamachi and D. Cutter, Opt. Commun. 22, 283 (1977).
25. K. Nagashima and T. Asakura, Atti Della Fondazione Giorgio Ronchi 33, 623 (1978).
26. K.B. Eisenthal, Chem. Phys. Letters 6, 155 (1970).
27. R.M. Anderson, R. Hochstrasser, H. Lutz and G.W. Scott J. Chem. Phys. 61, 2500 (1974).
28. R.H. Hochstrasser and A.C. Nelson, Opt. Commun. 18, 361 (1976).
29. U.K.A. Klein, R. Frey, A. Hanser and U. Gosele, Chem. Phys. Letters 41, 139 (1976).
30. J. Jortner and A. Ben-Reuven, Chem. Phys. Letters 41, 401 (1976).
31. I. Kaplan and J. Jortner, Chem. Phys. Letters 51, 1 (1977).

32. R. Katrarco, A. Ron and S. Speiser, Chem. Phys. Letters 52, 16 (1977).
33. I. Kaplan and J. Jortner, Chem. Phys. Letters 52, 202 (1977).
34. V.D. Kotzubanov, Yu. V. Naboikin, L.A. Ogurtsova, A.P. Podgornyi and P.S. Pokrovskaya, Optics and Spectroscopy 25, 406 (1969).
35. T. Urisu and K. Kajiyama J. Appl. Phys. 47, 3559 (1976).
36. F.P. Schafer, Dye Lasers, eds. F.P. Schafer (Springer-Verlag, 1977) p. 51.
37. K.H. Drexhage, Dye Lasers, eds. F.P. Schafer (Springer-Verlag, 1977) p. 160.

CHAPTER V

SUMMARY

Eventhough a large number of schemes have been proposed and developed for  $N_2$  laser pumped dye lasers the relatively low efficiency compelled the scientists to device new methods to improve the system efficiency. Energy transfer mechanism has been shown to be a convenient tool for the enhancement of efficiency of dye lasers. The present work covers a detailed study of the performance characteristics of a  $N_2$  laser pumped dye laser in the conventional mode and also, when pumped by the energy transfer mechanism.

For the present investigations a dye laser pumped by a  $N_2$  laser ( $\sim 200$  kW peak power) was fabricated. The grating at grazing incidence was used as the beam expanding device. At its best performance the system was giving an output peak power of 15 kW for a  $5 \times 10^{-3}$  M/l Rh-6 solution in methanol. The conversion efficiency was 7.5%. The output beam was having a divergence of 2 mrad and bandwidth 0.9 Å. Suitable modifications were suggested for obtaining better conversion efficiency and bandwidth.

The investigations on the output beam qualities have shown that the performance characteristics of the dye laser can be controlled by the system parameters. The output power varies linearly with the input pump power. The measured dependence of output power on the bandwidth

have shown that the conversion efficiency can be increased at the expense of bandwidth. The 3% conversion efficiency at a bandwidth of  $0.25 \text{ \AA}$  increases to 10.5% when the bandwidth is  $5 \text{ \AA}$ . The dye laser output pulse shape shows a close resemblance with that of the pumping  $\text{N}_2$  laser pulse.

The divergence measurements have clearly demonstrated the importance of the feedback mirror position with respect to the dye cell as a divergence deciding factor. If the feedback mirror is located within 8 cm from the centre of the dye cell, a diffraction limited beam divergence could not be obtained. Moreover, if the divergence is high the theoretical limit of the passive bandwidth of the system also could not be obtained. This effect is observed by measuring the bandwidth for different values of the beam divergences.

The degree of polarization of the output beam is found to be dependent on the type of dye molecules used. The  $10^\circ$  wedge angle of the dye cell windows with respect to the laser axis enhances the degree of polarization of the output beam. However, the suppression of one polarization component could not be obtained with this tilt angle. A completely polarized output beam may be obtained by the insertion of a glass plate in the cavity at a larger angle of incidence.

The concentration tuning range obtained for the various dyes investigated is found to be smaller than the earlier reported values. This is attributed to the low cavity and to the insufficient pump power to reach laser threshold.

The results of the investigations on mixed dye systems show the advantages of energy transfer mechanism in  $N_2$  laser pumped dye lasers. Even if it is impossible to pump a dye above threshold with  $N_2$  laser, laser action can be obtained by energy transfer mechanism as demonstrated in the case of Rh-6G -- Safranin T. Attempt made to lase Safranin T alone by  $N_2$  pumping was unsuccessful. Another important advantage of ETDL systems is the enhancement of efficiency. A substantial increase in the output power can be obtained by energy transfer mechanism if the concentrations of donor and acceptor are selected properly. The present investigations on Rh-6G - Rh-B and C 120 - Rh-6G systems show that a 1:1 ratio for the molar concentration of donor and acceptor is giving the maximum efficiency. A further increase in the donor concentration will affect the peak emission wavelength as well as the efficiency as a result of the formation of excited state complexes in the dye mixture. However, the 200% increase in the output power obtained for Rh-6G - Rh-B system with

a 1:1 ratio of the molar concentration of Rh-6G and Rh-B shows that ETDL system is more efficient than conventional dye lasers.